(12) INTERNATIONAL APPLICATION PUBLISHED UNDER THE PATENT COOPERATION TREATY (PCT)

(19) World Intellectual Property Organization
International Bureau

(43) International Publication Date
19 December 2024 (19.12.2024)

WIPO | PCT

(10) International Publication Number
WO 2024/258720 A2

(51) International Patent Classification:
Not classified

(21) International Application Number:
PCT/US2024/032681

(22) International Filing Date:
06 June 2024 (06.06.2024)

(25) Filing Language: English

(26) Publication Language: English

(30) Priority Data:
63/472,853 14 June 2023 (14.06.2023) US

(71) Applicant: **YALE UNIVERSITY** [US/US]; Two Whitney Avenue, New Haven, CT 06511 (US).

(72) Inventors: **LEE, Junseok**; 109 Church Street, Unit 404, New Haven, CT 06510 (US). **KIM, Changwoo**; Two Whitney Avenue, c/o Yale University, New Haven, CT 06510 (US). **FORTNER, John**; 291 Humphrey Street, Unit 4, New Haven, CT 0611 (US).

(74) Agent: **CALCAGNI, Jennifer A.**; Carmody Torrance Sandak & Hennessey, 195 Church Street, P.O. Box 1950, New Haven, CT 06509-1950 (US).

(81) Designated States *(unless otherwise indicated, for every kind of national protection available)*: AE, AG, AL, AM, AO, AT, AU, AZ, BA, BB, BG, BH, BN, BR, BW, BY, BZ, CA, CH, CL, CN, CO, CR, CU, CV, CZ, DE, DJ, DK, DM, DO, DZ, EC, EE, EG, ES, FI, GB, GD, GE, GH, GM, GT, HN, HR, HU, ID, IL, IN, IQ, IR, IS, IT, JM, JO, JP, KE, KG, KH, KN, KP, KR, KW, KZ, LA, LC, LK, LR, LS, LU, LY, MA, MD, MG, MK, MN, MU, MW, MX, MY, MZ, NA, NG, NI, NO, NZ, OM, PA, PE, PG, PH, PL, PT, QA, RO, RS, RU, RW, SA, SC, SD, SE, SG, SK, SL, ST, SV, SY, TH, TJ, TM, TN, TR, TT, TZ, UA, UG, US, UZ, VC, VN, WS, ZA, ZM, ZW.

(84) Designated States *(unless otherwise indicated, for every kind of regional protection available)*: ARIPO (BW, CV, GH, GM, KE, LR, LS, MW, MZ, NA, RW, SC, SD, SL, ST, SZ, TZ, UG, ZM, ZW), Eurasian (AM, AZ, BY, KG, KZ, RU, TJ, TM), European (AL, AT, BE, BG, CH, CY, CZ, DE, DK, EE, ES, FI, FR, GB, GR, HR, HU, IE, IS, IT, LT, LU, LV, MC, ME, MK, MT, NL, NO, PL, PT, RO, RS, SE, SI, SK, SM, TR), OAPI (BF, BJ, CF, CG, CI, CM, GA, GN, GQ, GW, KM, ML, MR, NE, SN, TD, TG).

Published:
— *without international search report and to be republished upon receipt of that report (Rule 48.2(g))*

(54) Title: ULTRA-HIGH CAPACITY MULTI-FUNCTIONAL NANOSCALE ADSORBENTS FOR PFAS TREATMENT

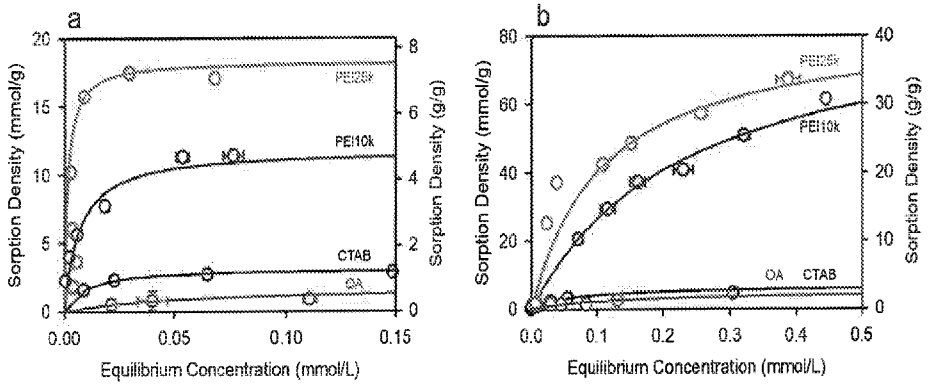

Fig. 1

(57) Abstract: Provided is an adsorbent for removing perfluoroalkyl and polyfluoroalkyl substances from an aqueous solution, including perfluoro-octanoic acid (PFOA), perfluoro-octane sulfonate (PFOS), shorter-chained perfluoroalkyl and polyfluoroalkyl substances, and combinations of foregoing. The adsorbent includes iron oxide nanocrystals, wherein the absorbent has an adsorption capacity for PFOA of at least 5000 mg/g or an adsorption capacity for PFOS of at least 25,000 mg/g. Also provided are methods of removing contaminants from an aqueous solution, wherein the contaminants include perfluoroalkyl and polyfluoroalkyl substances.

WO 2024/258720 A2

ULTRA-HIGH CAPACITY MULTI-FUNCTIONAL NANOSCALE ADSORBENTS FOR PFAS TREATMENT

CROSS REFERENCE TO RELATED APPLICATIONS

[0001] The present invention claims the benefit of U.S. Provisional Application Serial No. 63/472,853, filed on June 14, 2023, the subject matter of which is herein incorporated by reference in its entirety.

STATEMENT REGARDING FEDERALLY SPONSORED RESEARCH OR DEVELOPMENT

[0002] This invention was made with Government support under Grant No. EEC-1449500, awarded by the National Science Foundation. The U.S. Government has certain rights in the invention.

FIELD OF THE INVENTION

[0003] The present invention relates generally to high capacity multi-functional nanoscale adsorbents for treatments of perfluoroalkyl and polyfluoroalkyl substances and methods of using the same for treatment of these substances.

BACKGROUND OF THE INVENTION

[0004] Perfluoroalkyl and polyfluoroalkyl substances (PFAS) are pollutants of concern due to their long-term persistence in the environment and human health effects. PFAS have been industrially produced and used in numerous products such as fire-fighting foams, carpets, paints, and metal plating for decades, leading to wide spread environmental release. PFAS have been detected in surface, ground, drinking and waste waters at concentrations ranging from ca. 10 to 2,000 ng/L depending on the extent of release and distance from sources.

[0005] PFAS represent a broad class of organic chemicals that contain a hydrophobic fluorinated carbon chain and a polar end group, consisting of either sulfonate, carboxylate, alcohol, or sulfonamide. Due to their amphiphilic properties and high stability, PFAS were extensively used as surface coatings in textiles and apparel, paper and food packaging, and aqueous film-forming foams (AFFF) for fire suppression. As a consequence of fire fighter training exercises and fire response, among other uses, PFAS have been detected in groundwater at numerous DoD installations.

[0006] The U.S. Environmental Protection Agency (U.S. EPA) has proposed final National Drinking Water Regulation (NPDWR) for six PFAS compounds:

a. perfluoro-octanoic acid (PFOA);
b. perfluoro-octane sulfonate (PFOS));
c. perfluoro-hexane sulfonate (PFHxS);
d. perfluoro-nonanoic acid (PFNA);
e. hexafluoro-propylene oxide dimer acid(HFPO-DA); and
f. perfluoro-butane sulfonate (PFBS);

[0007] Among various PFAS species, long chain C-F compounds, including perfluorooctanoic acid (PFOA) and perfluorooctanesulfonic acid (PFOS), have been associated with numerous potential adverse health effects, and thus pose a risk upon exposure. The finalized legally enforceable levels, called Maximum Contaminant Levels (MCLs) to 4.0 parts per trillion (ppt, ng/L) for PFOA and PFOS, and 10 ppt for PFHxS, PFNA, and HFPO-DA, while mixtures containing two or more of PFHxS, PFNA, HFPO-DA, and PFBS has 1 of Hazard Index regulated. In addition, a number of states have proposed or adopted PFAS regulations with a maximum contaminant level as low as 10 ng/L. Due to their unique physicochemical properties, underpinned by strong carbon-fluorine (C-F) bonds, PFAS are highly stable in natural system and typically recalcitrant to conventional chemical and biological degradation processes.

[0008] Various advanced treatment technologies have been explored to treat PFAS in water, including electrochemical oxidation, photocatalysis, sulfate radical-based advanced redox process, thermal destruction, biological treatment, and other oxidative and reductive methods. Additional processes, including electron beam and plasma, have also been applied, with higher energy inputs. While several of these processes show promise to treat a range of PFAS, longer chain (and fluorine saturated) PFOA and PFOS remain difficult to destroy, with PFOS being the more recalcitrant of the two.

[0009] As an alternative to chemical and/or biological destruction, physical-based separation processes such as adsorption and membrane separation, can be highly effective in treating PFAS regardless of carbon chain length and head group functionality. Removal of PFAS by various adsorbents, including activated carbon, carbon nanotubes, anion-exchange resin, polymers, metals, and/or metal oxides, have been described. Further, PFAS concentration as a pretreatment step for eventual transformation/immobilization is necessary for many remediation scenarios (due to relatively low environmental PFAS concentrations and associated reaction thermodynamics). PFAS separation by various sorbents, including activated carbon, carbon nanotubes, anion-exchange resins, polymers, metals, and metal oxides, have been previously

described. To improve removal efficacy, additional treatment processes conditions have also been explored to augment physical adsorption, including bubbles/mixing, and heat. Further, hybrid composite materials and organic functionalization (modification) have also been demonstrated to enhance sorption performance. For these, depending on the material and PFAS properties, both electrostatic and hydrophobic interaction(s) between PFAS and the adsorbent material surface have been observed to be important. From this perspective, hybrid nanocomposite materials are a promising class of sorbents, which can offer high surface area(s) and flexible surface coating platforms with tunable (multi)functional groups, along with responsive cores (e.g. magnetic, reactive, etc.). Despite such potential and technical need, a predictive framework for advanced sorbent development and selection as a function of site conditions remains largely underdeveloped.

[0010] U.S. Pat. No. 11,148,119 to Fortner et al., the subject matter of which is herein incorporated by reference in its entirety, describes engineering nanoparticles for aqueous applicants and synthetic pathways to prepare manganese oxide, manganese ferrite, and manganese ferrite coated iron oxide nanocrystals with varied size and composition and especially for use for uranyl sorption and separation in water. The disclosure presents uranium sorption of the synthesized manganese ferrite nanocrystals in high cationic salts, such as ground water conditions containing sodium and calcium. However, there is no suggestion that such materials can be used for the treatment of PFAS nor how such materials can be evaluated and/or optimized for good effect.

[0011] U.S. Pat. No. 9,376,328 to Guardia Giros et al., the subject matter of which is herein incorporated by reference in its entirety, describes methods of making ferrite nanocrystals.

[0012] There remains a need in the art for the development of new adsorbent materials that have an affinity for the removal of PFAS and other contaminants from water.

SUMMARY OF THE INVENTION

[0013] It is an object of the present invention to develop new materials and describe their performance, through structure-function relationships, towards optimized PFAS separation(s) in both the aqueous and vapor phases. In addition, by controlling sorbent properties, high throughput experiments can be performed along with various analytical techniques to analyze, data that will specifically inform free energy relationships with regard to PFAS sorption as a function of sorbent properties, PFAS type/chemistry, and environmental conditions. Elucidating

fundamental partitioning processes will, in turn, provide informed, predictive relationships when selecting/designing optimal sorbents for site specific treatment (for both aqueous and vapor phase processes).

BRIEF DESCRIPTION OF THE DRAWINGS

[0014] Figures 1(a) and 1(b) depict PFOA and PFOS sorption isotherms on iron oxide nanocrystals with different surface coatings.

[0015] Figures 2(a) and 2(b) depict PFOA and PFOS sorption isotherms on iron oxide nanocrystals obtained via batch and QCM-D methods.

[0016] Figures 3(a)-(d) depict single and multi-sorption isotherms on polyethyleneimine coated iron oxide nanocrystals for PFOA and PFOS.

[0017] Figure 4 depicts thickness of the attached layer of PFOA and PFOS on the iron oxide nanocrystal coated Q-sensor.

[0018] Figures 5(a)-(d) depict PFOA and (B) PFOS sorption isotherm on PEI coated IONCs (Fe_3O_4@PEI25k) as a function of water chemistry.

[0019] Figures 6(a) and 6(b) depict effluent breakthrough curves for PFOA and PFOS in columns packed with IONCs (2.9 mg) treated 40-50 mesh Ottawa Sand (80 g).

[0020] Figure 7 depicts TEM images of monodisperse iron oxide nanoparticles (IONCs) and histograms of the size distribution of NCs.

[0021] Figures 8(a) and 8(b) depict hydrodynamic diameters and zeta potential of organic functionalized IONCs with polyethyleneimine, cetyltrimethylammonium bromide, and oleic acid.

[0022] Figure 9 depicts real time frequency responses of QCM-D for PFAS sorption on organic functionalized iron oxide nanocrystals (IONCs) coated Q-sensor.

[0023] Figures 10(a)-(f) depict frequency shift and slope with respect to the different concentration of IONCs with various surface coatings.

[0024] Figures 11(a) and 11(b) depict time dependent normalized sorption density of PEI coated IONCs (Fe_3O_4@PEI25k) for 0.6 mM of PFOA and PFOS.

[0025] Figures 12(a) and 12(b) depict real time deposition rates ($-f_{3\_slope}$) of PFOA and PFOS on IONCs with respect to the different surface coating (PEI25k, PEI10k, and CTAB).

[0026] Figures 13(a) and 13(b) depict frequency shift quartz crystal sensor (overtone = 3) with 0.6 mM of PFOA and PFOS solutions at pH 7.

[0027] Figures 14(a) and 14(b) depict PFOA and PFOS sorption isotherms on iron oxide nanocrystals (IONCs) obtained from mass of IONCs deposited on Q-sensor and mole of PFAS attached to IONCs via QCM-D.

[0028] Figure 15 depicts zeta potential of PEI coated IONCs with different molecular weight (25k and 10k) as a function of solution pH.

[0029] Figures 16(a) and 16(b) depict aggregation profiles of Fe_3O_4@PEI25k NCs in the presence of 1000 mM of NaCl and 1000 mM of $CaCl_2$ concentrations at pH 7.

[0030] Figures 17(a) and 17(b) depict normalized sorption density for PFOA and PFOS on Fe_3O_4@PEI25k NCs as a function of humic acid concentrations via QCM-D method.

[0031] Figure 18 depicts a diagram of the experimental system used for the column studies.

DETAILED DESCRIPTION OF THE PREFERRED EMBOMDIMENTS

[0032] The inventors of the present invention have discovered that one of the keys to enabling long-term, in situ PFAS removal are the use of nanoscale absorbents as described herein. The inventors of the present invention have designed and developed surface engineered, superparamagnetic iron oxide nanocrystals (IONCs) for the effective removal of PFAS in water. These PFAS may include, for example, shorter chained PFAS such as perfluorohexanoic acid (PFHxA), perfluorobutanoic acid (PFBA), perfluorohexanesulphonic acid (PFHxS), as well as PFOA and PFOS.

[0033] These materials are designed as composites with multiple material aspects, including a functional magnetic core and tunable surface coatings. As a core, iron oxide structures are high effective platform materials for amine-based polymers such as polyethyleneimine (PEI). The material is capable of maintaining enormous surface areas while begin scalable for synthesis.

[0034] These paramagnetic magnetite nanoparticles provide a unique advantage based on their ability to respond to an external magnetic field, thus allow for potential low energy and precise placement and/or recovery. In addition, iron oxide materials are low-cost, commercially available, non-toxic and stable over a range of environmental conditions likely to be encountered in groundwater and other sources of contaminated water.

[0035] As used herein, "a," "an," and "the" refer to both singular and plural referents unless the context clearly dictates otherwise.

[0036] As used herein, the term "about" refers to a measurable value such as a parameter, an amount, a temporal duration, and the like and is meant to include variations of +/-15% or less,

preferably variations of +/-10% or less, more preferably variations of +/-5% or less, even more preferably variations of +/-1% or less, and still more preferably variations of +/-0.1% or less of and from the particularly recited value, in so far as such variations are appropriate to perform in the invention described herein. Furthermore, it is also to be understood that the value to which the modifier " about" refers is itself specifically disclosed herein.

[0037] As used herein, spatially relative terms, such as "beneath," "below," "lower," "above," "upper" and the like, are used for ease of description to describe one element or feature's relationship to another element(s) or feature(s) as illustrated in the figures. Spatially relative terms may be intended to encompass different orientations of the device in use or operation in addition to the orientation depicted in the figures.

[0038] It is further understood that the terms "front" and "back" are not intended to be limiting and are intended to be interchangeable where appropriate.

[0039] As used herein, the terms "comprises" and/or "comprising," specify the presence of stated features, integers, steps, operations, elements, and/or components, but do not preclude the presence or addition of one or more other features, integers, steps, operations, elements, components, and/or groups thereof.

[0040] As described herein, the present invention relates generally to an adsorbent for removing perfluoroalkyl and polyfluoroalkyl substances from water, wherein the adsorbent comprises iron oxide nanocrystals. These iron oxide nanocrystals are surface engineered, superparamagnetic iron oxide nanocrystals and are demonstrated to effectively remove PFAS, including PFOA and PFOS from contaminated water, such as ground water.

[0041] The adsorbents described herein the absorbent can be constructed to have an adsorption capacity for perfluoro-octanoic acid (PFOA) of at least 2,000 mg/g, or at least 3,000 mg/g, or at least 4,000 mg/g or at least 5,000 mg/g or at least 6,000 mg/g or at least 7,000 mg/g or at least 7,500 mg/g. In addition, the adsorbents can be constructed to have an adsorption capacity for perfluoro-octane sulfonate (PFOS) of at least 20,000 mg/g, or at least 25,000 mg/g, or at least 30,000 mg/g , or at least 35,000 mg/g, or at least 40,000 mg/g, or at least 44,000 mg/g. In addition, the adsorbents can be constructed to have an adsorption capacity for perfluorohexanoic acid (PFHxA) of at least 2,000 mg/g, or at least 3,000 mg/g, or at least 4, 000 mg/g, or at least 5,000 mg/g or at least 6,000 mg/g or at least 6,500 mg/g. The adsorbents can also be constructed to have an adsorption capacity for perfluorobutanoic acid (PFHxA) of at least 2,000 mg/g, or at least 3,000 mg/g, or at least 4, 000 mg/g, or at least 5,000 mg/g or at least 5,500 mg/g. The

adsorbents can also be constructed to have an adsorption capacity for perfluorohexanesulphonic acid (PFHxA) of at least 2,000 mg/g, or at least 3,000 mg/g, or at least 4, 000 mg/g, or at least 5,000 mg/g or at least 5,500 mg/g or at least 6,000 mg/g.

[0042] As described herein, in one embodiment, the adsorbent comprises iron oxide nanocrystals that are coated with polyethyleneimine (PEI), preferably a highly branched PEI polymer.

[0043] PEI polymers have positively charge amine functionality along with hydrophobic sites that are energetically favorable for PFAS sorption. In addition, both linear and dendritic PEI polymers are either commercially available or can be formulated with a variety of molecular weights, branching degrees, and amine types (primary, secondary, tertiary amine groups) and ratios for sorption optimization for a given system, which system may be based, for example on PFAS type and/or water chemistry.

[0044] Moreover, based on the sorption mechanism, facile PFAS recovery is possible via a simple pH increase and/or ion exchange, and thus the composite materials described herein has a high potential for reuse as compared with other materials such as granulated activated carbon. This produces concentrated PFAS streams that are more economical and thermodynamically favorable to destructively treat.

[0045] As described below, the critical role of organic functional groups in the engineered IONCs on sorption behavior was evaluated.

[0046] Among the materials studied and evaluated, positively charged polyethyleneimine (PEI) coated IONCs showed ultra-high sorption capacities for both PFOA and PFOS due to favorable molecular interactions and high grafting densities as well as shorter chained PFAS such as perfluorohexanoic acid (PFHxA), perfluorobutanoic acid (PFBA), and perfluorohexanesulphonic acid (PFHxS).

[0047] For these, the effect of water chemistry, including solution pH, ionic composition and strength, and natural organic matter on sorption performance was studied in addition to bench-scale (sand) column studies.

[0048] The present invention also describes a quartz crystal microbalance with dissipation (QCM-D) method in order to fundamentally characterize interfacial PFAS adsorption processes in situ and in real time. This method provides rapid, accurate, and continuous response to system perturbations, such as changes in solution chemistry and sorbate composition and concentration. Such an approach allows for mechanistic understanding of competitive sorption dynamics, including molecular (sorbate) orientation, underpinning bulk behavior observations.

[0049] It is believed that the materials described herein can be designed and developed for a range of amine based (PEI), surface-associated polymers. Based thereon, it is an objective of the present invention to synthesize libraries of PEI-based (IONC) materials, considering molecular weight (MW) and conformation, along with amine site density (C:N ratios) and types (primary, secondary, tertiary amine groups) as explained in more detail below.

[0050] It is also believed that polymer properties and water chemistry play a role in governing PFAS sorption extent and kinetics. To evaluate these properties, a procedure was developed to evaluate developed sorbents (as a function of PFAS type and aqueous chemistries, through both traditional (batch isotherm) and high throughput approaches. High throughput experiments were performed with a quartz crystal microbalance (QCM), which allows for real time analysis of interfacial (sorption) processes with real-time, dynamic inputs.

[0051] It is also believed that the magnetic core materials (Fe_3O_4) and an (partially) electrostatic-based sorption mechanism, allow for composite material reuse. In particular, PFOA and PFOS, as well as shorter chained PFAS such as perfluorohexanoic acid (PFHxA), perfluorobutanoic acid (PFBA), perfluorohexanesulphonic acid (PFHxS), can be effectively (magnetically) separated from bulk solution and desorbed upon pH increase. PFAS recovery (upon sorption and separation) is explored based on (high) pH for PFAS recovery (i.e., from favorable (neutral pH) to unfavorable for PFAS association at high pH). Cycling potential and material stability were also evaluated for promising materials.

[0052] Magnetic recovery experiments were performed under low-magnetic field and described in terms of mass recovery per unit time for a given volume and particle concentration.

[0053] Promising sorbent materials believed to have enhanced gas phase PFAS sorption properties and vapor phase PFAS sorption (described as gas phase partitioning constants) were evaluated and quantified for each sorbent material. In particular, volatile PFAS (i.e., lower MW) molecules are evaluated for vapor phase sorption by both advanced sorbents and control materials, including activated carbon. Sorption properties of sorbent materials are explored as a function of PFAS type (MW, class, and head functionality) as well as environmental conditions (relative humidity).

[0054] Given the control of experimental parameters and material synthesis, along with a high throughput approach, the generated data sets reveal clear structure-function relationships based on free energy relationships. The present invention also provides methods for exploring specific data as a function of sorbent (e.g. PEI type and properties) and PFAS type (varied in MW,

isomers, and head group chemistry), along with aqueous chemistries, for free energy trends based on (partitioning-based) equilibrium calculations. Such data sets elucidate the relative roles (or magnitudes) of the considered variables and variable grouping(s).

[0055] As further described herein, the IONC materials of the present invention have ultra-high sorption capacities, are superparamagnetic, and are recyclable, with numerous uses per material unit. These materials are also scalable.

[0056] In one embodiment, the present invention also relates generally to a method of removing contaminants from an aqueous solution, wherein the contaminants comprise perfluoroalkyl and polyfluoroalkyl substances, the method comprising the steps of:

a) passing the aqueous solution containing contaminants through an adsorption column, wherein the adsorption column contains the adsorbent described herein; and

b) removing the treated aqueous solution from the adsorption column;

wherein the adsorbent adsorbs some or all of the contaminants present in the aqueous solution.

[0057] In one embodiment, the aqueous solution containing contaminants is passed through the adsorption column using a solvent delivery system. In one embodiment, the solvent delivery system may be an HPLC pump that is configured to pump the aqueous solution through the adsorption column at a pressure in the range of about 1 to about 20 atm.

[0058] In one embodiment, the aqueous solution containing contaminants comprises ground water or contaminated water.

[0059] In one embodiment, the aqueous solution containing contaminants has a pH in the range of about 2 to about 8.

[0060] In one embodiment, the method further comprises the step of regenerating the adsorbent, which may be accomplished by contacting the adsorbent with a aqueous solution at a pH of at or above about 10. In one embodiment, the solvent comprises water or any pH sensitive solvent and/or solvent combination that is pH sensitive and/or active.

[0061] In one embodiment the present invention also relates generally to a system comprising an adsorption column, cartridge, or housing containing the adsorbent described herein, wherein the adsorbent is capable of removing contaminants from an aqueous solution, wherein the contaminants comprise perfluoro-octanoic acid, perfluoro-octane sulfonate, shorter-chained perfluoroalkyl and polyfluoroalkyl substances, and combinations of foregoing.

[0062] An example of a system in accordance with the invention is shown in Figure 18, which depicts an experimental system used for the column studies in the Examples. As shown in Figure 18, the aqueous solution is pumped into a bottom of an adsorption column containing the adsorbent described herein using a HPLC pump. The treated aqueous solution is then removed from the top of the column.

[0063] A summary of adsorption capacities for PFAS and PFOS on various adsorbents is provided below in Table 1. As seen in Table 1 the adsorption capacity for both PFAS and PFOS using an adsorbent of the present invention is much higher than the adsorption capacity of any other adsorbent studied.

Table 1. Adsorption capacities for PFOA and PFOS on various adsorbents

Adsorbate	Adsorbent	Water matrix	pH	Adsorption Capacity	
				mg/g	mmol/g
PFOA	Powdered activated carbon (PAC)	DI water	3	426	1.03
	Granular activated carbon (GAC)	DI water	5	476	1.15
	Polyacrylonitrile fiber-derived activated carbon fibers (PACFs)	DI water	5	302	0.73
	Single wall carbon nanotubes (SWCNT)	DI water	6	80	0.19
	Modified titanate nanotubes	DI water	2-10	1,100	2.66
	Anion exchange resin (IRA910)	DI water	6	1,440	3.47
	Anion exchange resin (IRA400)	DI water	2-12	1,210	2.92
	Polyaniline nanotubes (PANTs)	DI water	2-9	1,100	2.66
	Quaternized cotton	DI water	3-10	1,240	2.99
	Animated rice husk	DI water	5	1,030	2.49
	Metal organic framework (MOF)	DI water	5	500	1.2
	Magnetic nanoparticles (NP)	DI water	7	62.5	0.15
	Fe_3O_4@PEI25k	DI water	7	7,580	18.3
PFOS	PAC	DI water	3	440	0.88
	GAC	DI water	5	1,160	2.32
	PACFs	DI water	5	760	1.52
	SWCNT	DI water	6	560	1.12
	SWCNT	DI water		710	1.42
	PANTs	DI water	2-9	1,650	3.30
	Anion exchange resin (IRA67)	Actual WW	3	2,750	5.5
	Anion exchange resin (IRA67)	DI water	3	2,500	5.0
	Animated polyacrylonitrile fibers (APANFs)	DI water	3	7,500	15.0
	Chitosan-based molecularly imprinted polymer (MIP)	DI water	3-10	1,460	3.53
	Crosslinked chitosan	DI water	3	2,500	6.04
	Quaternized cotton	DI water	3-10	1,750	3.50
	Animated rice husk	DI water	5	1,330	2.65
	Porous aromatic framework (PAF-45)	DI water	3	5,850	11.7
	Magnetic fluorinated vermiculite	DI water	6	1,130	2.26
	Fe_3O_4@PEI25k	DI water	7	44,410	88.8

[0064] Fig. 1(a) presents PFOA and Fig. 1(b) presents PFOS sorption isotherm on IONCs with different organic (surface) coating positively charged PEI (25k and 10k of MW) and cetyltrimethylammonium bromide (CTAB), and negatively charged oleic acid (OA), respectively. All experiments were performed at pH 7.

[0065] Figs. 2(a) and 2(b) present PFAS sorption isotherms on IONCs determined by both batch sorption (circle dot and solid line) and QCM-D methods with such correction factors. QCM-D results are obtained by multiplying a QCM-D correction factor with sorbent density. Overall, corrected sorption density from QCM-D (reverse triangle dot and dotted line) match well with batch sorption results, which highlights QCM-D as a feasible tool to determine sorption behavior(s) in real time without complicated analysis/measurement procedures of target adsorbates (e.g. LC-MS).

[0066] Multi-sorbate tests considering both PFOA and PFOS were performed to determine competitive effects on isotherm behavior(s) using Fe_3O_4@PEI25k NCs (highest performing material). Sorption isotherms for multi-sorbate systems (both PFOA and PFOS) and single-sorbate are presented in Figs. 3(a) and 3(b). Figs. 3(a) PFOA and 3(b) PFOS present single- and multi-sorption isotherms on PEI coated IONCs for (single-sorbate systems and multi-sorbate systems (PFOA and PFOS. Multi-sorption tests were performed with the same initial concentration of both PFOA and PFOS from 0.02 to 0.1 mmol/L at pH 7. (c-d) Time dependent frequency and dissipation shift (overtone n = 3) of the IONCs coated Q-sensor with introducing both PFOA and PFOS sequentially, and vice versa, by QCM-D analysis.

[0067] Interestingly, PFOA sorption on IONCs was significantly hindered in the presence of PFOS, for which maximum sorption capacity was 18.3 mmol g^{-1} (PFOA as the single sorbate) and 7.0 mmol g^{-1} for multi-sorbate systems, respectively. The sorption density for PFOS was also considerably decreased in the presence of PFOA (88.8 mmol g^{-1} for single (PFOS as single sorbate) and 20.4 mmol g^{-1} for multi-sorbate systems, respectively). It is believed that this is simply competitive adsorption, with differential adsorption affinities based on PFAS head group. Sorption density of PFOA on IONCs in the multi-sorbate system also decreased in the case of higher equilibrium concentrations (above 0.1 mmol/L), further indicating that PFOA molecules adsorbed on IONCs are readily exchanged by PFOS.

[0068] To further evaluate sorption preference between PFOA and PFOS, real time sorption behavior was evaluated using the QCM-D method described above. To do this, either 0.6 mM of PFOA or PFOS solutions was introduced over IONCs coated Q-sensor sequentially. As shown in

Figs. 3(c) and 3(d), frequency and dissipation shifts associated with PFOA and PFOS sorption events were observed, indicating attachment (sorption) of PFAS on IONCs. After stabilization, we then switched the solutions from PFOA to PFOS and PFOS to PFOA, respectively. Additional frequency and dissipation shifts in the system were observed with newly introduced PFOS, indicating molecular exchange and/or additional sorption (Fig. 3(c)), while no changes in both frequency and/or dissipation were observed when PFOA was introduced to a system with PFOS previously sorbed (Fig. 3(d)). These observations support batch results, described above, further implicating the key role of the PFAS head group with regard to sorption behavior.

[0069] The carboxylic head group of PFOA has a lower pKa value than PFOS and shows a higher affinity to positively charged IONCs, resulting in higher Langmuir adsorption constants (k). In comparison, the sulfonic group of PFOS results in a relatively lower k value due to lower bulk affinity compared PFOA. However, PFOS has three different resonance structure(s) which, when taken together, allows for overall more favorable interactions.

[0070] To explore this directly, the thickness of PFAS layer, as a function of PFAS type was demonstrated using the Voigt model via QCM-D analysis. With all variables held constant (IONC, water chemistry, etc.) except for PFAS type, Fig. 4 shows the thickness of the attached layer of PFOA and PFOS on the IONC coated Q-sensor obtained as calculated by the Voigt model via frequency shift (*f*) and dissipation (*D*) during PFAS sorption. As seen in Fig. 4, a difference between PFOA and PFOS sorbed layers is about 5 angstrom (Å), indicating the orientation of sorbed PFAS is fundamentally different based on the functional head groups. For these, PFOS tends to be more vertically aligned on the surface of IONCs because of resonance structure of sulfonic group, while PFOA tends to align in a more horizontal fashion, which is also supported by the maximum sorption values observed (i.e., higher sorption density is possible with vertically oriented PFOS). Differences in sorbed orientation between PFOA and PFOS may also contribute to the relative recalcitrance of PFOS relating to steric hindrance and/or active site distance from a reactive material surface(s).

[0071] To understand how water chemistry affects PFAS sorption behavior, PFAS sorption was evaluated using Fe_3O_4@PEI25k as a function of solution pH, ionic strength and type, and NOM in water. Figs. 5(a) and 5(b) shows that higher sorption densities were observed under both acidic (pH 4.0) and neutral (pH 7.0) conditions, compared to basic conditions (pH 10.0), as expected. The maximum sorption capacity was 14.7 mmol g^{-1} at pH 4.0, 18.3 mmol g^{-1} at pH 7.0,

and 9.2 mmol g^{-1} at pH 10.0 for PFOA, and 58.8 mmol g^{-1} at pH 4.0, 83.5 mmol g^{-1} at pH 7.0, and 38.5 mmol g^{-1} at pH 10.0 for PFOS, respectively.

[0072] Fig. 15 shows the zeta potential of PEI coated IONCs with different molecular weights (25k and 10k) as a function of pH. The observed decrease in sorption at higher pH values was attributed a decrease in surface zeta potential, and thus, a lower electrostatic affinity for negatively charged PFAS molecules as shown in Fig. 15. Thus, it appears that sorption can effectively be performed under both acidic and neutral conditions.

[0073] The effect of ionic strength and type on PFAS sorption was also evaluated using Fe_3O_4@PEI25k NCs via batch sorption experiments at pH 7. Here NaCl, $CaCl_2$, $MgCl_2$, were evaluated along with a synthetic groundwater (SGW) and compared with ultrapure water (UPW). Synthetic groundwater was prepared and the composition is summarized in Table 2.

Table 2. Ionic composition of synthetic groundwater.

Ion	Na^+	Ca^{2+}	Mg^{2+}	HCO^{3-}	Cl^-	HPO_4^{2-}	SiO_3^{2-}
Conc. (mM)	10.4	2.5	1.6	8.2	8.2	0.1	1

[0074] Fig. 5(a) (PFOA) and 5(b) (PFOS) depict sorption isotherms on PEI coated IONCs (Fe_3O_4@PEI25k) as a function of pH (4.0, 7.0, and 10.0). Fig. 5(c) (PFOA) and 5(b) (PFOS) depict sorption isotherms with different water chemistry of ultrapure water (UPW), NaCl, $CaCl_2$, $MgCl_2$, and synthetic groundwater (SGW), respectively. Total ionic strength for all solutions was adjusted to be identical with SGW.

[0075] As shown in Figs. 5(c) and 5(d), sorption capacities for both PFOA and PFOS decreased in the presence of all salts evaluated and the synthetic groundwater. The maximum sorption densities for PFOA were observed to be 18.3, 5.7, 5.1, 5.7, and 14.3 mmol g^{-1} for ultrapure water, NaCl, $CaCl_2$, $MgCl_2$, and synthetic groundwater, respectively, and 83.5, 54.3, 69.0, 73.7, and 31.5 mmol g^{-1} toward PFOS for ultrapure water, NaCl, $CaCl_2$, $MgCl_2$, and synthetic groundwater, respectively. Competitive effects of ionic species on PFAS sorption performance were observed, with similar or higher hindrance observed for NaCl compared to $CaCl_2$ and $MgCl_2$. Despite these interferences, material performance under real world conditions remains considerably higher than other reported sorbents which only considered pure water (i.e. best case scenario) as shown in Table 1.

[0076] Fig. 16(a) and 16(b) depicts an aggregation profile of Fe_3O_4@PEI25k NCs in the presence of 1000 mM of NaCl (Fig. 16(a)) and 1000 mM of $CaCl_2$ (Fig. 16(b)) concentrations at pH 7. For all suspensions evaluated, no IONC aggregation was observed under any condition evaluated as shown in Figs. 16(a) and 16(b), thus minimizing the loss of surface area as a confounding performance factor.

[0077] PFAS sorption capacities also decreased in the presence of NOM (0–0.5 mg/L). To quantify this process, the role of humic acid (HA) concentration on sorption density via QCM-D analysis was evaluated. Figs. 17(a) and (b) depict normalized sorption density for PFOA (Fig. 17(a)) and PFOS (Fig. 17(b)) on Fe_3O_4@PEI25k NCs as a function of humic acid (HA) concentrations via QCM-D method. As shown in Figs. 17(a) and 17(b), sorption densities decreased with increase of HA concentration. Humic acid, with a large cation exchange capacity, readily competes in bulk with positively active sites on IONCs for PFAS sorption, as observed by others for negatively charged pollutants.

[0078] To demonstrate application potential, effluent breakthrough curves obtained following the injection of solutions containing PFOA or PFOS into columns packed IONC treated 40-50 mesh Ottawa sand (80 g) are shown in Figs. 6(a) and 6(b). For the PFOA column study, a solution containing 100 µg/L PFOA in 10 mM NaCl was introduced for 10 pore volumes (PVs), with no detectable levels of PFOA observed in effluent samples. To assess the limiting adsorptive capacity of the IONC-treated sand, the influent concentration of PFOA was then increased to 10 mg/L (considered as a very high environmental PFAS concentration), which resulted in detection of PFOA after approximately 31 PVs. The concentration of PFOA increased steadily to a relative concentration (C/C_0) of 0.83 after 39 PVs, and reached the influent concentration ($C/C_0 = 1$) at 49 PVs (Fig. 6(a)). Over the course of the experiment, a total of 5.16 mg of PFOA were retained, which corresponds to 5.37 mM PFOA per g of IONC (2.34 mg total IONC in the column), in line with batch sorption study results.

[0079] For the PFOS column study, a solution containing 100 µg/L PFOS in 10 mM NaCl was introduced for approximately 10 PVs with no detectable levels of PFOS observed in the column effluent. Similar to the PFOA column study, the concentration of PFOS in the influent solution was then increased to 10 mg/L and PFOS was subsequently detected in the effluent after approximately 23 PVs, and increased steadily to the influent concentration ($C/C_0 = 1$) after 39 PVs (Fig. 6(b)). Overall, a total of 6.34 mg of PFOS was retained in the IONC-treated column, which corresponds to 5.18 mM PFOS per g of IONCs (2.45 mg total in the column), also in line

with batch studies. When compared to control columns conducted with clean 40-50 mesh Ottawa sand, retention, thus treatment, of PFOA or PFOS in IONC-treated columns increased by more than three orders of magnitude.

EXAMPLE:

Preparation of Organic (Surface) Functionalized IONCs

[0080] Iron oxide nanocrystals (IONCs) were synthesized by iron precursor decomposition at high temperature. Synthesized 20 nm NCs were then functionalized with different organic surfactants using probe sonication via ligand exchange and encapsulation methods. Branched PEI, CTAB, and OA were used as surface stabilizers. 0.4 mL of NCs in hexane solution was mixed with particular amounts of surface stabilizer in 5 mL of ultrapure water (18.2 MΩ·cm, Millipore) by applying a probe sonicator (UP50H, Hielscher) at 80% amplitude and full cycle for 10 min. The remaining hexane in solution was removed by putting the solution under the fume hood for 24 h. To remove excess surfactants the solution was filtered by ultrafiltration membrane (cellulose, 100kDa MWCO, Millipore) with stirring, followed by syringe filtration (0.22 μm PES, Millipore). The concentration of functionalized IONCs in water was measured by inductively coupled plasma mass spectroscopy (ICP-MS, Elan DRC-e, Perkin Elmer).

Sorption Isotherms

[0081] Engineered IONCs (10 mg/L NC) were tested for PFAS sorption in the range of 0.01 to 0.2 mmol/L of PFOA and 0.01 to 0.6 mmol/L of PFOS concentrations at different pH conditions (4.0, 7.0, and 10.0 ± 0.2). Solution pH was adjusted using HNO_3 and NaOH firstly after setting the sorption tests, and further adjusted and/or confirmed again during the sorption experiments (after 4 h). At equilibrium (after 24 h), the NCs were separated using ultracentrifuge (Sorvall WX 80, Thermo Scientific) at 50,000 rpm for 2 h, and the remaining concentrations of PFAS were measured by ultra-performance liquid chromatograph (UPLC-MS/MS) (Waters Corporation, Milford, MA).

[0082] The measured sorption density (mmol of adsorbed PFAS per mass of NCs in the sample) as a function of equilibrium concentration of PFAS (mmol/L) was fitted by both Langmuir and Freundlich sorption isotherms. The Langmuir isotherm was obtained by following equation:

$$q_e = \frac{q_{max} k C_e}{(1 + k C_e)}$$

where q_e is sorption density at equilibrium (mmol/g), q_{max} is the maximum sorption density, k is Langmuir sorption constant (L/mmol), and C_e is equilibrium concentration of PFAS (mmol/L). And the Freundlich isotherm was determined as follow:

$$q_e = KC_e^{1/n}$$

where K and n are Freundlich sorption constants. Competitive sorption experiments were conducted with the initial concentrations of both PFOA and PFOS from 0.02 to 0.1 mmol/L at pH 7. The solution pH was twice adjusted, and other experimental conditions and procedures were identical to the single-sorbate sorption isotherm tests.

Quartz Crystal Microbalance with Dissipation (QCM-D)

[0083] Quartz crystal microbalance was performed with dissipation (QCM-D, Q-sense E4, Biolin Scientific) measurements by frequency (f) and energy dissipation (D) of silica coated Q-sensor (QSX-303, Q-sense). The mass deposited on the crystal surface per unit area (Δm) was determined by measuring frequency shift of the crystal using Sauerbrey relationship as described below:

$$\Delta m = -\frac{C}{n}\Delta f_n$$

where C is the crystal constant (17.7 ng/(cm^2·Hz) for 5 MHz quartz crystal), n is the overtone number (1, 3, 5, 7, 9, 11, and 13), and Δf_n is frequency shift at overtone number n. Considering the stability of the instrument, third overtone was used for the analysis of data in this study. For all measurements, the flowrate of solutions was maintained at 0.1 mL/min and the temperature inside the unit at 20.0°C.

Determination of PFAS Sorption Behavior via QCM-D Study

[0084] Real time frequency shifts were obtained to determine PFAS sorption isotherm on IONCs using QCM-D as following sequence. First, positively charged IONCs (PEI and CTAB coated) were introduced to quartz crystal sensor. Different concentrations of NCs were tested to determine the concentration of NCs that can fully cover the Q-sensor. Sensors were saturated with NCs (solution) for 20 min, and subsequently flowed with ultrapure water to stabilize and eliminate any loosely associated NCs to the Q-sensor. After stabilization, PFAS solutions were introduced, which showed additional frequency shifts regard to mass of PFAS attached to the IONCs on sensor. Sorption isotherm is determined from the deposited mass of PFAS and IONCs on the Q-sensor, which calculated from frequency shift through Sauerbrey equation.

QCM-D Factor

[0085] To compensate the underestimation of sorption capacity in QCM-D measurement due to attachment of water molecules on Q-sensor, QCM-D correction factor for sorption density was applied and the QCM-D factor was calculated as described below.

$$\text{QCM-D factor} = \frac{Mass\ of\ (NCs + Water)}{Mass\ of\ NCs}$$

The mass of sorbed water is calculated from the difference of volume between NC core size and hydrodynamic diameter by multiplying density of water.

Thickness of Deposited Layer on the Q-sensor

[0086] The thickness of deposited layer was calculated by analyzing the recorded Δf and ΔD data through Voigt model. The resulting thickness (δ) was obtained by equation as below.

$$\delta = \sqrt{\frac{2\eta_0}{\omega\rho_0}}$$

where η is shear viscosity, ω is angular velocity ($\omega = 2\pi f$), and ρ is density.

Column Studies

[0087] Column experiments were performed to quantify the adsorption of PFOA or PFOS by IONCs under dynamic flow conditions. A suspension of IONCs (20 mL at 145 mg/L) was mixed with 80 g of 40-50 mesh Ottawa sand and allowed to dry at 60°C for 48 hours. The IONC-treated sand, which contained approximately 2.9 mg IONC, was then packed into a borosilicate glass column (2.5 cm i.d. × 10 cm length) in 1-cm increments, flushed with CO_2 gas for 1 h, and then saturated with degassed background electrolyte solution (10 mM NaCl) at a flow rate of 1.0 mL/min. The resulting pore volume (PV) of the water-saturated columns was approximately 20.5 mL. Non-reactive tracer tests were performed after water saturation of each column by injecting 3.5 PVs of 10 mM NaBr followed by 3.5 PVs of 10 mM NaCl using a Chrome Tech P-010 isocratic pump (Apple Valley, MN) at a flow rate of 0.12 mL/min, which corresponds to a pore-water velocity of approximately 1 m/day. A schematic diagram of the experimental system used for the column studies is shown in Fig. 18.

[0088] To assess the ability of the IONC-treated sand to sequester PFOA and PFOS, aqueous solutions containing either PFOA (100 µg/L) or PFOS (100 µg/L) in 10 mM NaCl were injected into the columns at a flow rate of 0.12 mL/min. After approximately 10 PV, the influent concentration of PFOA or PFOS was increased from 100 µg/L to 10 mg/L to determine to

maximum adsorption capacity of the IONCs. Effluent samples were collected continuously using a Spectra/Chrom® CF-2 fraction collector (Spectrum Chemical Mfg. Corp., New Brunswick, NJ) to monitor for PFAS breakthrough. Effluent samples were filtered through 0.45μm GE Healthcare Whatman™ GD/X Glass Micro Fiber (GMF) syringe filter (GE Healthcare, Chicago, IL) and diluted to an appropriate concentration range prior to analysis using a Waters Xevo™ TQ-S Micro triple quadrupole mass spectrometer (LC–MS/MS).

[0089] Fig. 7 depicts transmission electron microscope (TEM) images of monodisperse iron oxide nanoparticles (IONCs) and histograms of the size distribution of NCs. Average diameter of NCs was measured using Image-Pro 6.0 with over a thousand counted. Scale bar is 50 nm. The TEM micrographs in Fig. 7 show as synthesized, monodisperse IONCs, and their size distribution (20.9 ± 1.5 nm, 55.3 m^2/g of core specific surface area). IONC crystalline structure is well matched with magnetite (Fe_3O_4) (JCPDS card #190629) by XRD analysis, which is superparamagnetic in this size range. Superparamagnetic functionality was included as part of the material platform for potential applications in low energy, precise (magnetic) separations from larger volumes and/or as a safety feature with regard to unwanted release. IONCs were subsequently surface functionalized with a series organic coatings, including branched polyethyleneimine (PEI) with different molecular weights (10kDa and 25kDa), cetyltrimethylammonium bromide (CTAB), and oleic acid (OA), all allowing for phase transfer into water, termed here as Fe_3O_4@PEI, Fe_3O_4@CTAB, and Fe_3O_4@OA, respectively. Surface functionalized IONCs were characterized in water by dynamic light scattering (DLS) to measure hydrodynamic diameter and surface zeta potential at pH 7 ± 0.2.

[0090] Figs 8(a) and 8(b) depict hydrodynamic diameters (Fig. 8(a)) and zeta potential (Fig. 8(b)) of organic functionalized IONCs with polyethyleneimine (PEI), cetyltrimethylammonium bromide (CTAB), and oleic acid (OA) at pH 7.0 ± 0.2. As tabulated in Fig. 8(a), the hydrodynamic diameter is 63.0 ± 2.4 nm for Fe_3O_4@PEI25k, 40.4 ± 2.8 nm for Fe_3O_4@PEI10k, 25.8 ± 3.0 nm for Fe_3O_4@CTAB, and 32.6 ± 3.6 nm for Fe_3O_4@OA. Zeta potential of Fe_3O_4@PEI25k, Fe_3O_4@PEI10k, Fe_3O_4@CTAB, and Fe_3O_4@OA is 54.3 ± 1.3, 57.4 ± 1.5, 29.1 ± 4.9, and -24.2 ± 1.8 mV, respectively. Coating analysis, including grafting densities and composition are presented in Table 3.

[0091] Batch surface coating dependent PFAS sorption tests were performed at pH 7 ± 0.2. As shown in Fig. 1, positively charged Fe_3O_4@PEI nanocrystals (NCs) demonstrate significantly higher sorption density compared to negatively charged Fe_3O_4@OA NCs. The maximum

sorption capacity of PFOA and PFOS was 18.3 mmol PFOA g^{-1} NC and 88.8 mmol PFOS g^{-1} NC for Fe_3O_4@PEI25k, and 11.9 mmol PFOA g^{-1} NC and 83.5 mmol PFOS g^{-1} NC for Fe_3O_4@PEI10k, respectively. Negatively charged Fe_3O_4@OA have significantly lower sorption capacities for both PFOA and PFOS (1.83 mmol PFOA g^{-1} NC and 6.58 mmol PFOS g^{-1} NC). As highlighted in Table 1, Fe_3O_4@PEI materials described in this study demonstrate some of the highest sorption capacities reported to date. This is believed to be not only a function favorable amine — anion PFAS head group, in which electrostatic interactions coupled with a large number of active (amine sites) as part of the PEI dendritic structure as shown in Table 3, but also due to high particle (aqueous) stability, thus maximum surface area/site availability as shown in Figs. 8(a) and 8(b). Comparatively, Fe_3O_4@PEI25k is observed to have higher sorption capacities than Fe_3O_4@PEI10k despite having a similar number of amine groups. This is likely due to a combination of relatively higher grafting (mass) density of PEI25k and a higher amine to carbon ratio compared to PEI10k.

Table 3. Organic loading on the nanocrystals.

Nanocrystals	Molecular weight of coating material	Total organic carbon (ppm of carbon)[α]	Number of carbon per nanocrystal	Number of amine groups per carbon[β, γ]	Number of amine groups per nanocrystal	Number of molecules per nanocrystal
Fe_3O_4@PEI25k	25,000	63 ± 1.3	690,306	0.5[β]	345,153	297
Fe_3O_4@PEI10k	10,000	57 ± 0.7	627,729	0.5	313,864	676
Fe_3O_4@CTAB	364.45	6.3 ± 0.1	685,526	0.037[γ]	25,364	25,364

[α]Total organic carbon (TOC) for organic functionalized iron oxide nanocrystals (10 ppm Fe).

[β]Number of amine groups per carbon of PEI coated IONCs was obtained by considering repeat unit of multi branched PEI structure.

[γ]Number of amine groups per carbon of CTAB functionalized IONCs was obtained based on an assumption of full surfactant encapsulation.

[0092] All batch sorption isotherms were well matched with a Langmuir adsorption model as shown in Table 4 below and then a Freundlich isotherm with the corresponding sorption constant (k) for PFOA was calculated to be much higher than that of PFOS regardless of sorbent. Interestingly, PFOS is observed to have higher maximum sorption density (Q_{max}) compared to PFOA, for all material combinations explored. For example, the k and Q_{max} values on

Fe_3O_4@PEI25k are 657 L/mmol and 18.3 mmol/g for PFOA, and 4.22 L/mmol and 88.8 mmol/g for PFOS, respectively. This difference indicates that PFAS functional group(s) significantly contribute to the sorption behavior as PFOA and PFOS having identical 'tail' structure. It is believed that the PFOA carboxyl group, with a lower pKa value (~ 5) than the PFOS sulfonic group (~ 7), has a lower interaction energy. Amine – carboxyl interactions typically have a low enthalpy (ΔH) value (-21.41 kJ/mol) compared to amine – sulfonic interactions (-42.81 kJ/mol).[50,51] Despite this, PFOS is observed to have a much higher maximum sorption density (Q_{max}) than PFOA. To explain this, the average geometrical orientation of the sorption event must thus differ (PFOA vs. PFOS) if all other variables are held constant, which is further explored and discussed below.

Table 4. Sorption isotherm constants and regression data for Langmuir and Freundlich adsorption isotherm models.

Target	Adsorbents	Langmuir Isotherm			Freundlich Isotherm		
		q_{max} (mmol/g)	k (L/mmol)	R^2	K_f[a]	n	R^2
PFOA	Fe_3O_4@PEI25k	18.3	657	0.99	41.9	4.28	0.88
	Fe_3O_4@PEI10k	11.9	148	0.95	29.9	2.92	0.98
	Fe_3O_4@CTAB	3.14	112	0.99	4.16	5.36	0.90
	Fe_3O_4@OA	1.83	16.5	0.70	3.60	1.94	0.89
PFOS	Fe_3O_4@PEI25k	88.8	4.22	0.99	98.6	1.73	0.99
	Fe_3O_4@PEI10k	83.5	9.27	0.99	88.5	3.20	0.95
	Fe_3O_4@CTAB	6.58	16.3	0.99	7.02	3.10	0.97
	Fe_3O_4@OA	5.30	6.89	0.61	16.0	1.17	0.75

[a]Unit of K_f is $(mmol/g)(L/mmol)^{1/n}$.

[0093] To better understand fundamental sorption dynamics, a quartz crystal microbalance with dissipation (QCM-D) monitoring technique was developed to observe real time, in situ sorption behavior of PFAS. Fig. 9 depicts real time frequency responses of QCM-D for PFAS sorption on organic functionalized iron oxide nanocrystals (IONCs) coated Q-sensor. For this, a stable, monolayer of IONCs was arranged at the sensor interfaces so that varied aqueous solutions can be introduced sequentially and equilibrated, including changes in water chemistry and PFAS concentration/type as shown in Fig. 9.

[0094] Figs. 10(a)-(f) show the frequency shift and slope with respect to the different concentration of IONCs with various surface coatings; CTAB (Figs. 10(a) and 10(b)), PEI25k (Figs. 10(c) and 10(d)), and PEI10k (Figs. 10(e) and 10(f)), respectively. Figs. 10(a)-(f) show the

kinetics (slope of frequency shift) of IONC deposition and sensor surface saturation (i.e. monolayer coverage) at or above 5 ppm of concentration of NCs. Once stabilized IONCs demonstrate relative fast responses upon introducing PFAS solutions and reached equilibrium within minutes. These results are consistent with the batch sorption isotherm and kinetic tests for both PFOA and PFOS using IONCs as set forth in Figs. 11(a) and 11(b), which depict time dependent normalized sorption density of PEI coated IONCs (Fe3O4@PEI25k) for 0.6 mM of PFOA (Fig. 11(a) and PFOS (Fig. 11(b).

[0095] To further understand PFAS sorption kinetics on IONCs, the slope of the frequency shift (f_{slope}) was calculated from the data obtained during QCM-D sorption experiments. Since the frequency shift (Δf) is proportional to a change in mass (Δm) on the crystal surface, the rate of Δf change is equivalent to the rate of mass change on the crystal surface (i.e., the rate of PFAS attachment or release). Thus, the PFAS sorption rate (kinetics) can be determined by calculating the slope of frequency shift (f_{slope}). Figs. 12(a) and 12(b) depict real time deposition rates ($-f_{3\_slope}$) of PFOA (Fig. 12(a)) and PFOS (Fig. 12(b)) on IONCs with respect to the different surface coating (PEI25k, PEI10k, and CTAB). As shown Figs. 12(a) and 12(b), Fe_3O_4@CTAB NCs showed highest value of f_{slope}, followed by Fe_3O_4@PEI10k and Fe_3O_4@PEI25k, which is inversely proportional to the hydrodynamic diameter of IONCs. It is expected that the thicker PEI (and more dense) surface coating layer requires more time for PFAS to fully sorb which is likely due to mass transfer limitations, while showing overall higher sorption densities due to relatively more binding sites.

[0096] Based on both frequency shifts from flowing IONCs and PFAS solutions to Q-sensor, I was determined that both PFOA and PFOS sorption density of IONCs using deposited mass via the Sauerbrey equation. Figs. 13(a) and 13(b) show frequency shift of quartz crystal sensor (overtone = 3) with 0.6 mM of PFOA (Fig. 13(a)) and PFOS (Fig. 13(B)) solutions at pH 7. It was confirmed no PFAS was directly attached to quartz crystal sensor without IONCs as set forth in Figs. 13(a) and 13(b), thus any observed frequency shift in the presence of PFAS is due to its association with IONCs.

[0097] Fig. 14 details sorption isotherms for both PFOA and PFOS for IONCs with different surface coatings (PEI25k, PEI10k, and CTAB) as calculated by mass per IONC (mass) via QCM-D. The initial calculated sorption density obtained from QCM-D showed relatively lower values than those from batch sorption tests . No correction factor was applied here to consider water sorption. Frequency shifts can be observed with the release of sorbed water associated with

certain polymers, thus interfering with sorbate association measurements. To address this issue, a correction factor was developed based on calculated mass of water associated with IONCs.

[0098] PFOA and PFOS concentrations were measured along with their corresponding C-labeled internal standards. A Waters ACQUITY ultra performance liquid chromatograph coupled with a Waters Xevo triple quadrupole mass spectrometer (UPLC-MS) (Waters Corporation, Milford, MA) was used and the injection volume was 10 µL. Solvent A contained 95% DI water and 5% methanol with 2 mM ammonium acetate. Solvent B contained 100% methanol with 2 mM ammonium Acetate. All solvents were prepared with LC-MS grade, purchased from Honeywell Burdick & Jackson (Muskegon, MI). The gradient started with 90% A and 10% B and held for 1 min, then ramped to 15% A and 85% B at 5min, then 0% A and 100% B at 5.1 min, maintained at 100% B until 7 min and ramped back to 90% A and 10% B at 7.5 min.

[0099] The eluent was then held at 90% A and 10% B until the end of the 10 min run. Column temperature was 50°C and source temperature was 150°C. Desolvation temperature was 350°C and desolvation gas flow was 650°C. Analytes were separated on a Waters BEH C-18 column (1.7 µm dia., 2.1 × 50 mm^2) at a flow rate of 0.4 mL/min with an eluent gradient containing 2 mM ammonium acetate in water or methanol. The mass spectrometer was operated in negative electrospray ionization (ESI-) with multiple reaction monitoring (MRM). The method was able to detect 40 PFAS, precursors and C labeled standards with a total run time of approximately 10 min and detection limits ranging from 5 to 20 ng/L.

[0100] **Additional embodiments:**

[0101] **Clause 1:** An adsorbent for removing perfluoroalkyl and polyfluoroalkyl substances from an aqueous solution, wherein the adsorbent comprises iron oxide nanocrystals, wherein the absorbent has an adsorption capacity for perfluoro-octanoic acid (PFOA) of at least 5000 mg/g or an adsorption capacity for perfluoro-octane sulfonate (PFOS) of at least 25,000 mg/g.

[0102] **Clause 2:** The adsorbent of Clause 1, wherein the adsorbent has an adsorption capacity for PFOA of at least 6,000 mg/g, preferably an adsorption capacity for PFOA of at least 7,000 mg/g, more preferably an adsorption capacity for PFOA of at least 7,500 mg/g.

[0103] **Clause 3:** The adsorbent of Clause 1 wherein the adsorbent has an adsorption capacity for PFOS of at least 30,000 mg/g, preferably an adsorption capacity for PFOS of at least 40,000 mg/g, more preferably an adsorption capacity for PFOS of at least 44,000 mg/g.

[0104] **Clause 4:** The adsorbent according to any of Clauses 1-3, wherein the iron oxide nanocrystals are coated with a positively charged polymer.

[0105] **Clause 5:** The adsorbent according to Clause 4, wherein the positively charged polymer is a positively charged polyethyleneimine polymer having a molecular weight of at least 8,000 g/mol or at least 10,000 g/mol or at least 15,000 g/mol or at least 20,000 g/mol or at least 25,000 g/mol.

[0106] **Clause 6:** The adsorbent according to Clause 5, wherein the polyethyleneimine polymer is a branched polyethyleneimine polymer.

[0107] **Clause 7:** The adsorbent according to Clause 5 or Clause 6, wherein the polyethyleneimine-coated iron oxide nanocrystals have a number of amine groups per nanocrystal of at least 300,000 or at least 325,000.

[0108] **Clause 8:** The adsorbent according to any of Clauses 1 to 7, wherein the adsorbent is superparamagnetic.

[0109] **Clause 9:** The adsorbent according to any of Clauses 1 to 8, wherein the adsorbent may be regenerated.

[0110] **Clause 10:** A method of removing contaminants from an aqueous solution, wherein the contaminants comprise perfluoroalkyl and polyfluoroalkyl substances, the method comprising the steps of:

a. passing the aqueous solution containing contaminants through an adsorption column, wherein the adsorption column contains the adsorbent of any of Clauses 1 to 9; and
b. removing the treated aqueous solution from the adsorption column;

wherein the adsorbent adsorbs some or all of the contaminants present in the aqueous solution.

[0111] **Clause 11:** The method according to Clause 10, wherein the aqueous solution is pumped through the adsorption column at a pressure in the range of 1-10 atm.

[0112] **Clause 12:** The method according to Clause 10 or Clause 11, wherein the aqueous solution comprises ground water or contaminated water.

[0113] **Clause 13:** The method according to any of Clauses 10 to 12, wherein the aqueous solution has a pH in the range of about 2 to about 8.

[0114] **Clause 14:** The method according to any of Clauses 10 to 13, wherein the perfluoroalkyl and polyfluoroalkyl substances are selected from the group consisting of perfluoro-octanoic acid, perfluoro-octane sulfonate, shorter-chained perfluoroalkyl and polyfluoroalkyl substances, and combinations of foregoing.

[0115] **Clause 15:** The method according to Clause 14, wherein the shorter-chained perfluoroalkyl and polyfluoroalkyl substances are selected from the group consisting of perfluorohexanoic acid (PFHxA), perfluorobutanoic acid (PFBA), perfluorohexanesulphonic acid (PFHxS), and combinations of the foregoing.

[0116] **Clause 16:** The method according to any of Clauses 10 to 15, further comprising the step of regenerating the adsorbent, wherein the adsorbent is regenerated by contacting the adsorbent with a solvent at a pH of at or above about 10.

[0117] **Clause 17:** A system comprising an adsorption column, cartridge, or housing containing the adsorbent of any of Clauses 1-9, wherein the adsorbent is capable of removing contaminants from an aqueous solution, wherein the contaminants comprise perfluoro-octanoic acid, perfluoro-octane sulfonate, shorter-chained perfluoroalkyl and polyfluoroalkyl substances, and combinations of foregoing.

WHAT IS CLAIMED IS:

1. An adsorbent for removing perfluoroalkyl and polyfluoroalkyl substances from an aqueous solution, wherein the adsorbent comprises iron oxide nanocrystals, wherein the absorbent has an adsorption capacity for perfluoro-octanoic acid (PFOA) of at least 5000 mg/g or an adsorption capacity for perfluoro-octane sulfonate (PFOS) of at least 25,000 mg/g.

2. The adsorbent of claim 1, wherein the adsorbent has an adsorption capacity for PFOA of at least 6,000 mg/g.

3. The adsorbent of claim 2, wherein the adsorbent has an adsorption capacity for PFOA of at least 7,000 mg/g.

4. The adsorbent according to claim 3, wherein the adsorbent has an adsorption capacity for PFOA of at least 7,500 mg/g.

5. The adsorbent of claim 1 wherein the adsorbent has an adsorption capacity for PFOS of at least 30,000 mg/g.

6. The adsorbent of claim 5, wherein the adsorbent has an adsorption capacity for PFOS of at least 40,000 mg/g.

7. The adsorbent according to claim 6, wherein the adsorbent has an adsorption capacity for PFOS of at least 44,000 mg/g.

8. The adsorbent according to claim 1, wherein the iron oxide nanocrystals are coated with a positively charged polymer.

9. The adsorbent according to claim 8, wherein the positively charged polymer is a positively charged polyethyleneimine polymer having a molecular weight of at least 8,000 g/mol or at least 10,000 g/mol or at least 15,000 g/mol or at least 20,000 g/mol or at least 25,000 g/mol.

10. The adsorbent according to claim 9, wherein the polyethyleneimine polymer is a branched polyethyleneimine polymer.

11. The adsorbent according to claim 9, wherein the polyethyleneimine-coated iron oxide nanocrystals have a number of amine groups per nanocrystal of at least 300,000 or at least 325,000.

12. The adsorbent according to claim 1, wherein the adsorbent is superparamagnetic.

13. The adsorbent according to claim 1, wherein the adsorbent may be regenerated.

14. A method of removing contaminants from an aqueous solution, wherein the contaminants comprise perfluoroalkyl and polyfluoroalkyl substances, the method comprising the steps of:

    a. passing the aqueous solution containing contaminants through an adsorption column, wherein the adsorption column contains the adsorbent of any of claims 1 to 12; and
    b. removing the treated aqueous solution from the adsorption column;

    wherein the adsorbent adsorbs some or all of the contaminants present in the aqueous solution.

15. The method according to claim 14, wherein the aqueous solution is pumped through the adsorption column at a pressure in the range of 1-10 atm.

16. The method according to claim 14, wherein the aqueous solution comprises ground water or contaminated water.

17. The method according to claim 14, wherein the aqueous solution has a pH in the range of about 2 to about 8.

18. The method according to claim 14, wherein the perfluoroalkyl and polyfluoroalkyl substances are selected from the group consisting of perfluoro-octanoic acid, perfluoro-

octane sulfonate, shorter-chained perfluoroalkyl and polyfluoroalkyl substances, and combinations of foregoing.

19. The method according to claim 18, wherein the shorter-chained perfluoroalkyl and polyfluoroalkyl substances are selected from the group consisting of perfluorohexanoic acid (PFHxA), perfluorobutanoic acid (PFBA), perfluorohexanesulphonic acid (PFHxS), and combinations of the foregoing.

20. The method according to claim 14, further comprising the step of regenerating the adsorbent, wherein the adsorbent is regenerated by contacting the adsorbent with a solvent at a pH of at or above about 10.

21. A system comprising an adsorption column, cartridge, or housing containing the adsorbent of any of claims 1-13, wherein the adsorbent is capable of removing contaminants from an aqueous solution, wherein the contaminants comprise perfluoro-octanoic acid, perfluoro-octane sulfonate, shorter-chained perfluoroalkyl and polyfluoroalkyl substances, and combinations of foregoing.

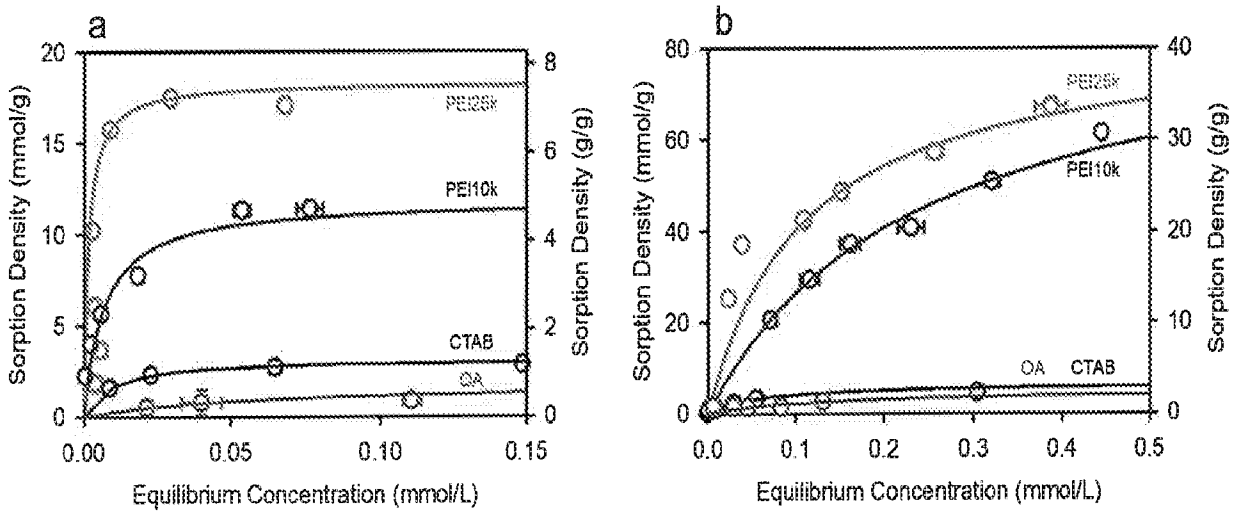
a
b
Sorption Density (mmol/g)
Sorption Density (g/g)
Equilibrium Concentration (mmol/L)
PEI25k
PEI10k
CTAB
OA

Fig. 1

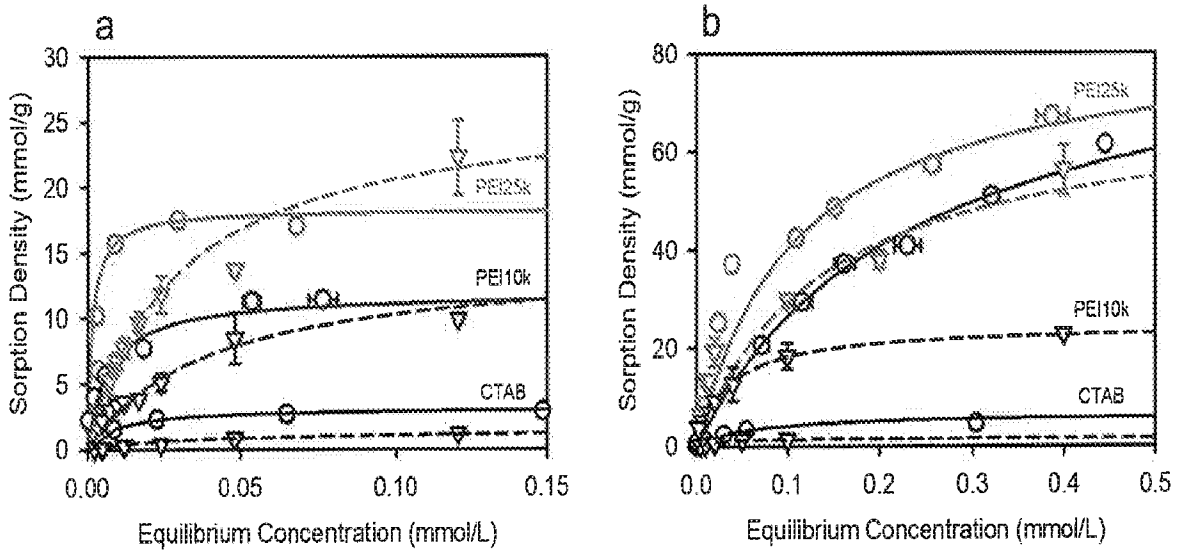
a
b
Sorption Density (mmol/g)
Equilibrium Concentration (mmol/L)
PEI25k
PEI10k
CTAB

Fig. 2

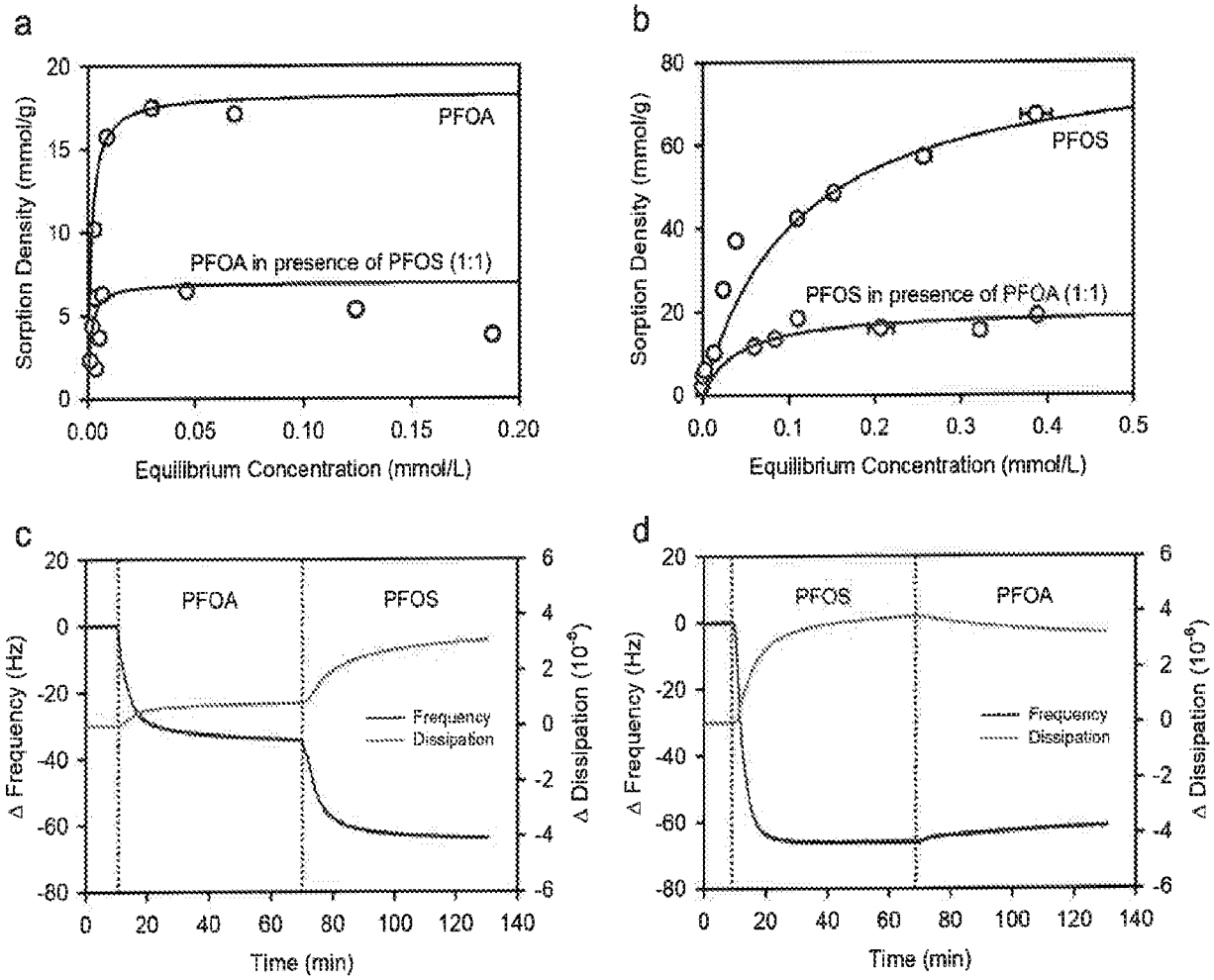
a
Sorption Density (mmol/g)
PFOA
PFOA in presence of PFOS (1:1)
Equilibrium Concentration (mmol/L)
b
Sorption Density (mmol/g)
PFOS
PFOS in presence of PFOA (1:1)
Equilibrium Concentration (mmol/L)
c
PFOA
PFOS
Frequency
Dissipation
Δ Frequency (Hz)
Δ Dissipation (10⁻⁶)
Time (min)
d
PFOS
PFOA
Frequency
Dissipation
Δ Frequency (Hz)
Δ Dissipation (10⁻⁶)
Time (min)

Fig. 3

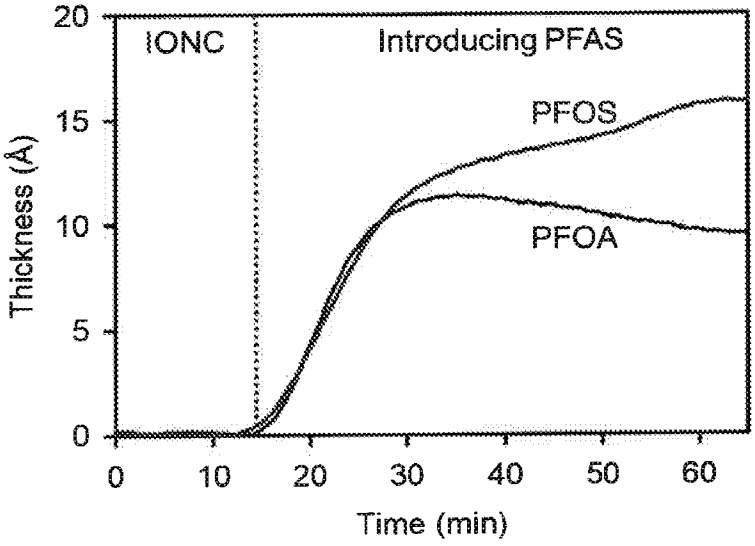
20
15
10
5
0
Thickness (Å)
IONC
Introducing PFAS
PFOS
PFOA
0
10
20
30
40
50
60
Time (min)

Fig. 4

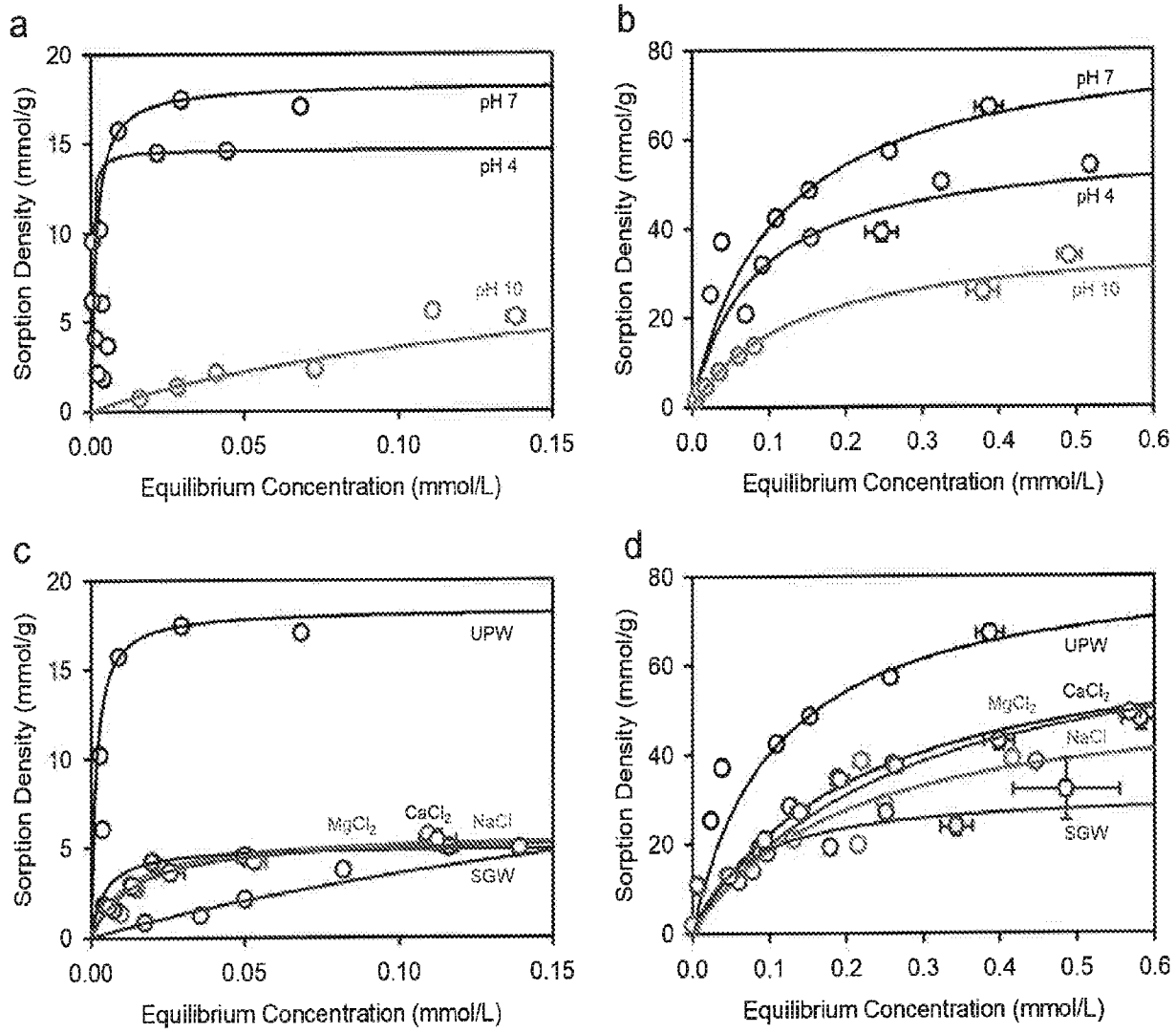
a
Sorption Density (mmol/g)
Equilibrium Concentration (mmol/L)
pH 7
pH 4
pH 10
b
Sorption Density (mmol/g)
Equilibrium Concentration (mmol/L)
pH 7
pH 4
pH 10
c
Sorption Density (mmol/g)
Equilibrium Concentration (mmol/L)
UPW
MgCl2
CaCl2
NaCl
SGW
d
Sorption Density (mmol/g)
Equilibrium Concentration (mmol/L)
UPW
MgCl2
CaCl2
NaCl
SGW

Fig. 5

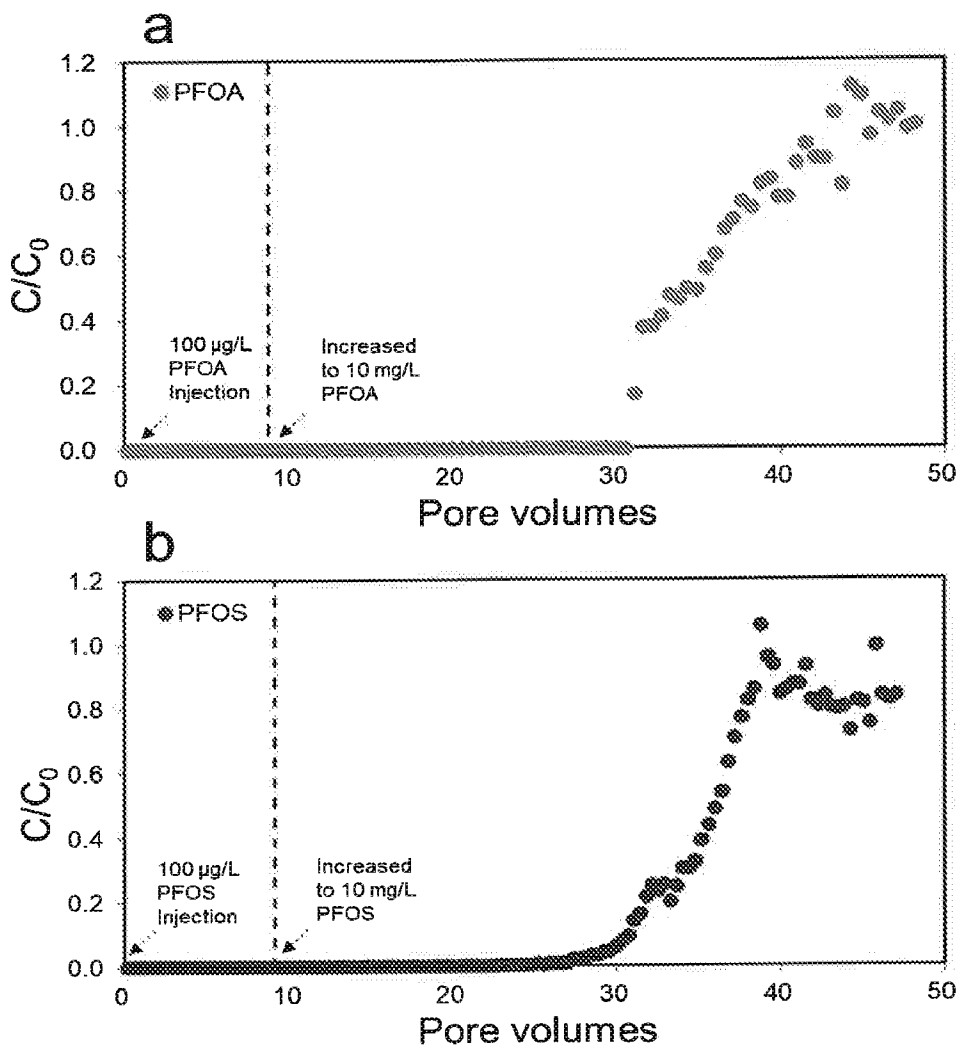
a
PFOA
C/C0
100 µg/L PFOA Injection
Increased to 10 mg/L PFOA
Pore volumes
b
PFOS
C/C0
100 µg/L PFOS Injection
Increased to 10 mg/L PFOS
Pore volumes

Fig. 6

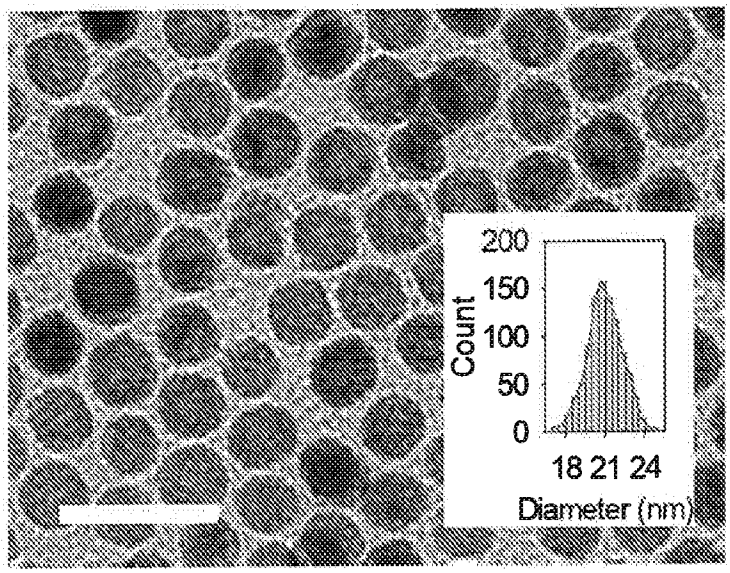
200
150
100
50
0
Count
18 21 24
Diameter (nm)

Fig. 7

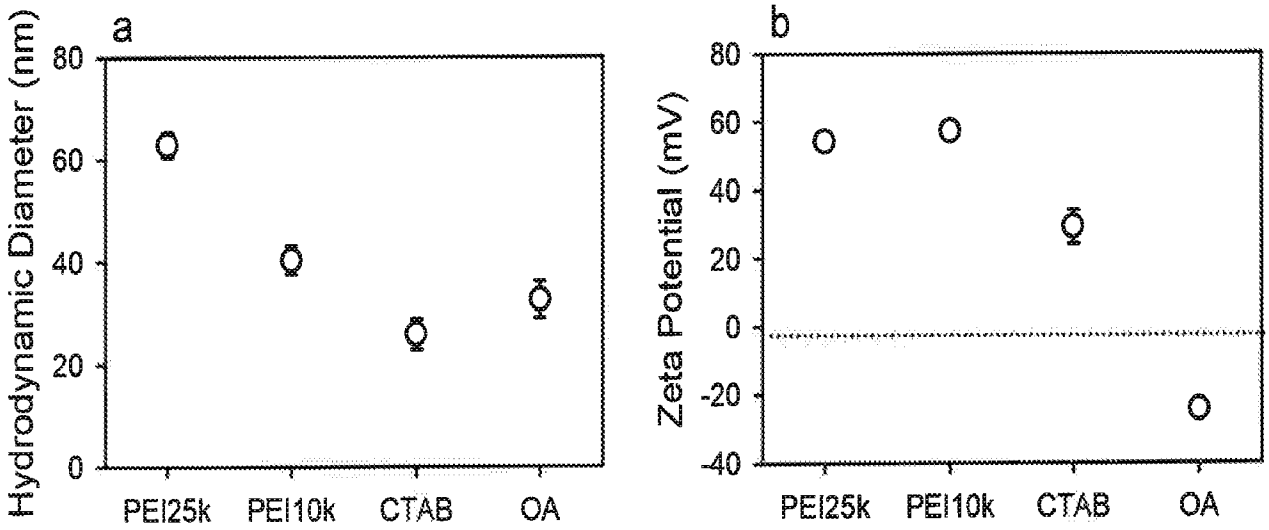
a
Hydrodynamic Diameter (nm)
80
60
40
20
0
PEI25k
PEI10k
CTAB
OA
b
Zeta Potential (mV)
80
60
40
20
0
-20
-40
PEI25k
PEI10k
CTAB
OA

Fig. 8

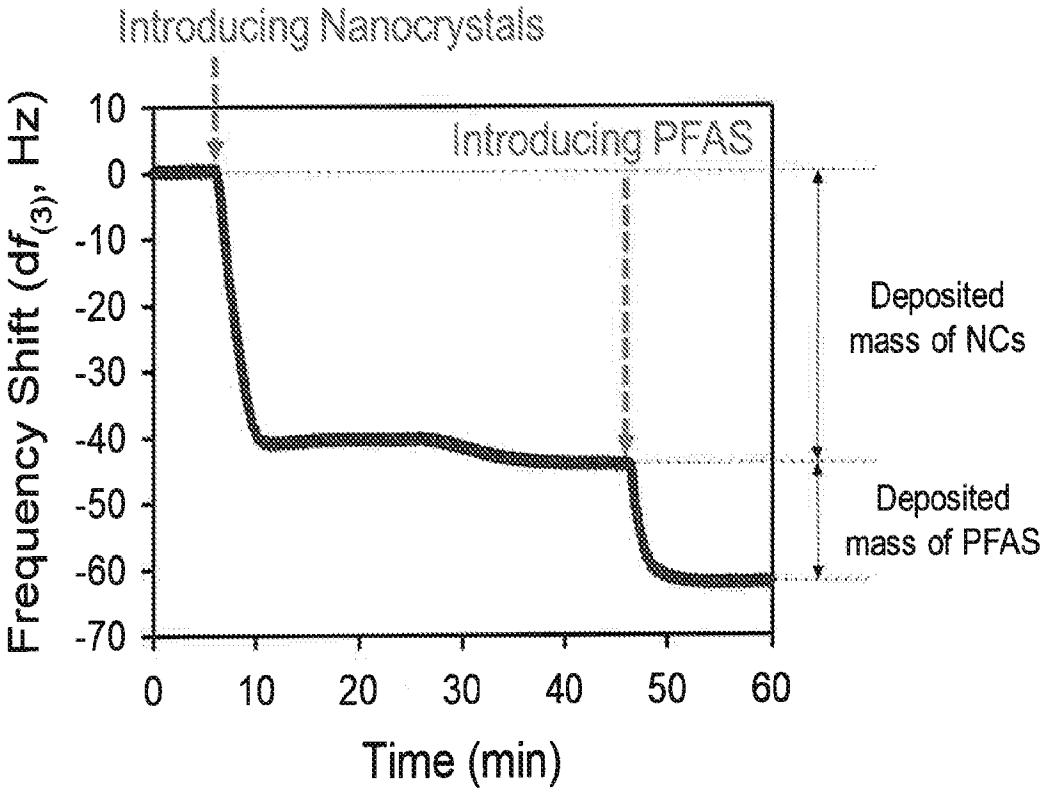
Introducing Nanocrystals
Introducing PFAS
Deposited mass of NCs
Deposited mass of PFAS
Frequency Shift ($df_{(3)}$, Hz)
10
0
-10
-20
-30
-40
-50
-60
-70
0
10
20
30
40
50
60
Time (min)

Fig. 9

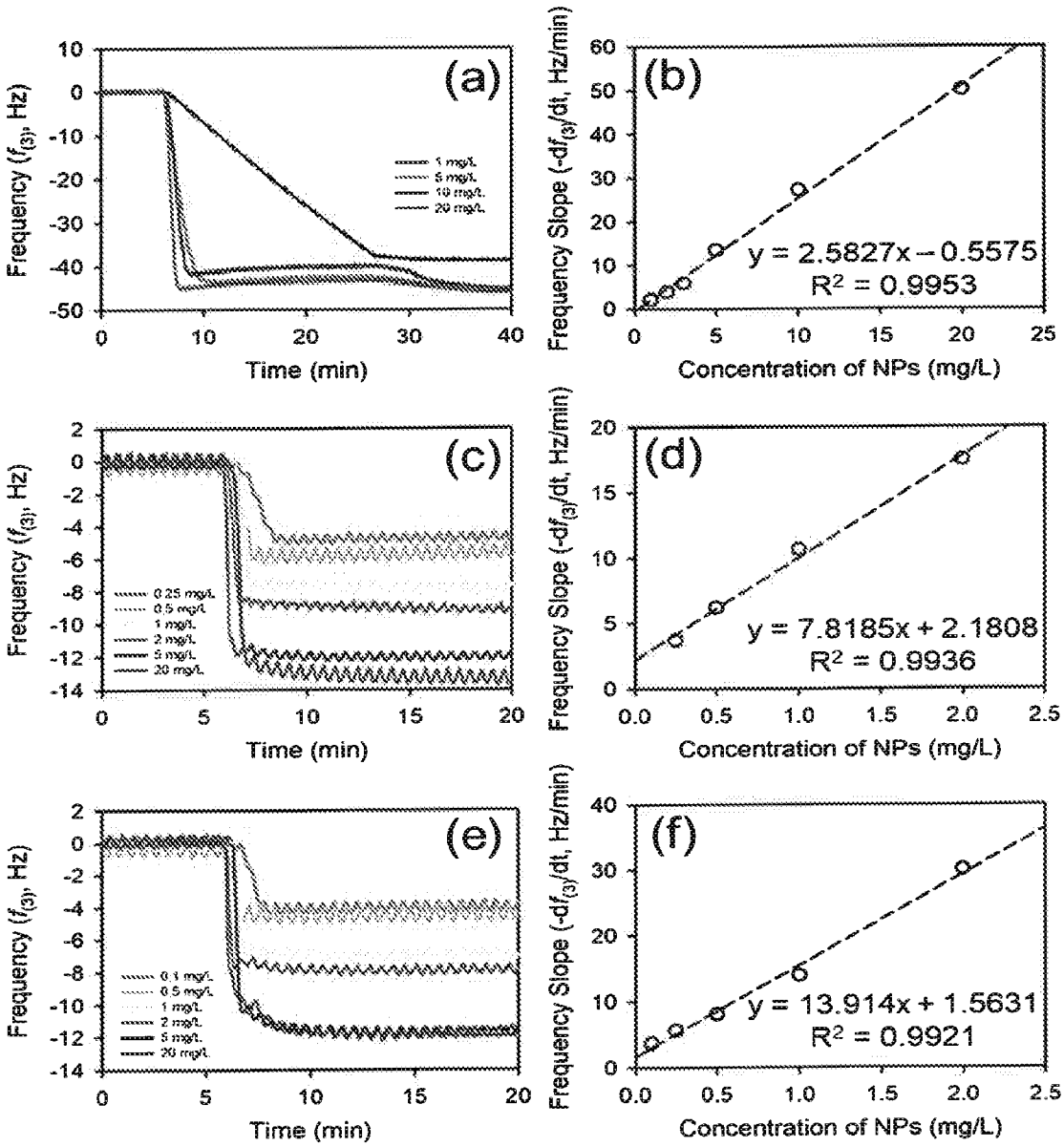
(a)
Frequency ($f_{(3)}$, Hz)
Time (min)
1 mg/L
5 mg/L
10 mg/L
20 mg/L
(b)
Frequency Slope ($-df_{(3)}/dt$, Hz/min)
Concentration of NPs (mg/L)
y = 2.5827x − 0.5575
R^2 = 0.9953
(c)
Frequency ($f_{(3)}$, Hz)
Time (min)
0.25 mg/L
0.5 mg/L
1 mg/L
2 mg/L
5 mg/L
20 mg/L
(d)
Frequency Slope ($-df_{(3)}/dt$, Hz/min)
Concentration of NPs (mg/L)
y = 7.8185x + 2.1808
R^2 = 0.9936
(e)
Frequency ($f_{(3)}$, Hz)
Time (min)
0.1 mg/L
0.5 mg/L
1 mg/L
2 mg/L
5 mg/L
20 mg/L
(f)
Frequency Slope ($-df_{(3)}/dt$, Hz/min)
Concentration of NPs (mg/L)
y = 13.914x + 1.5631
R^2 = 0.9921

Fig. 10

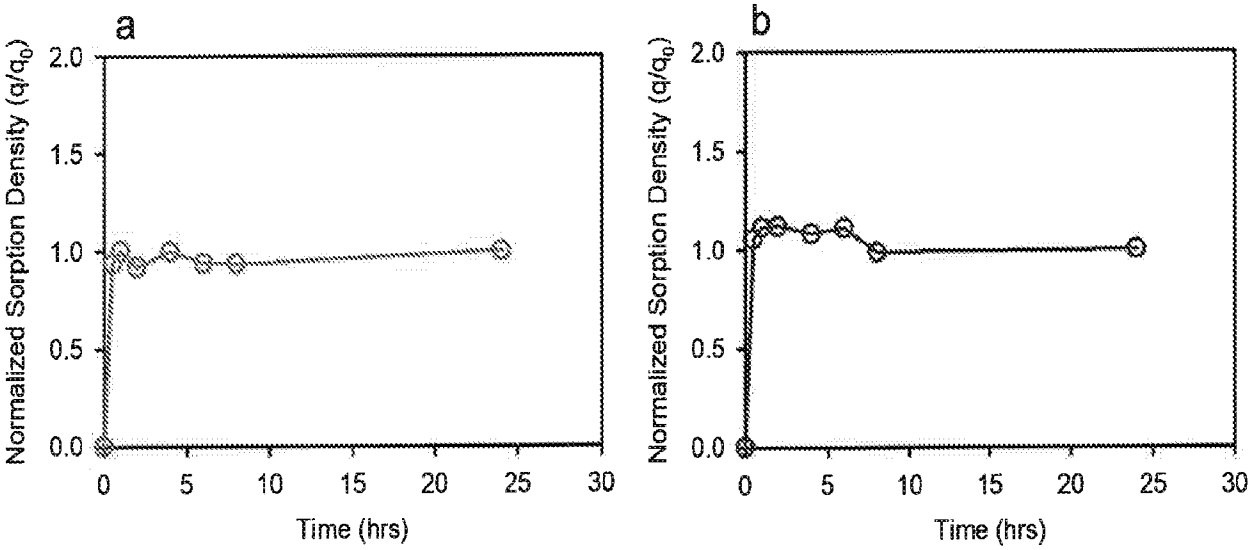
a
b
Normalized Sorption Density (q/q0)
Time (hrs)
0.0
0.5
1.0
1.5
2.0
0
5
10
15
20
25
30

Fig. 11

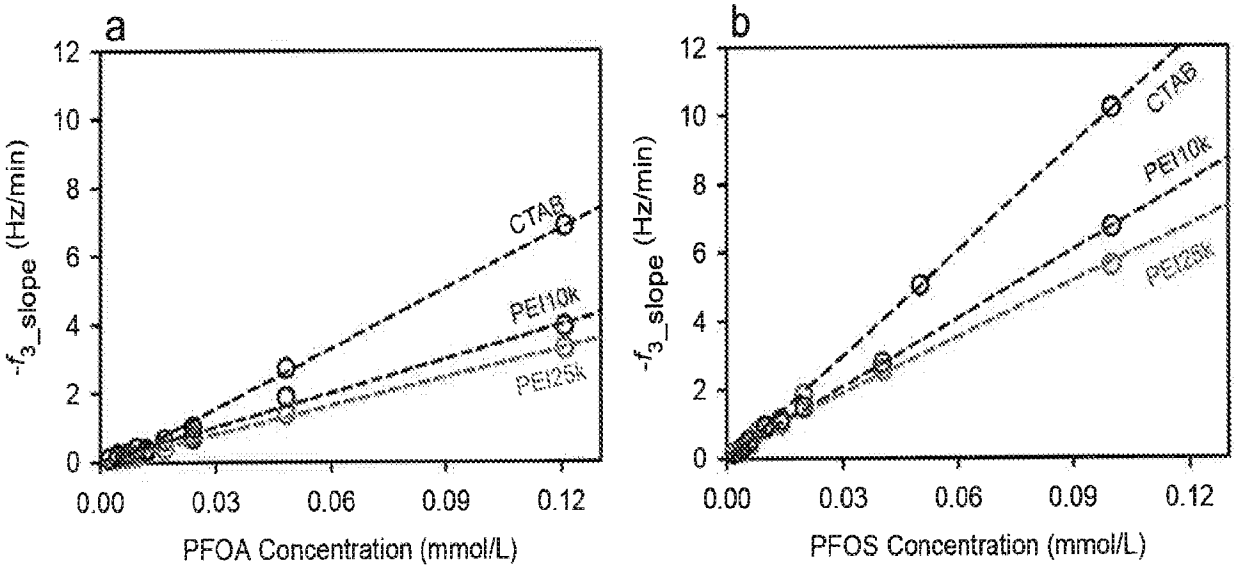
a
b
-f3_slope (Hz/min)
PFOA Concentration (mmol/L)
PFOS Concentration (mmol/L)
CTAB
PEI10K
PEI25K
0
2
4
6
8
10
12
0.00
0.03
0.06
0.09
0.12

Fig. 12

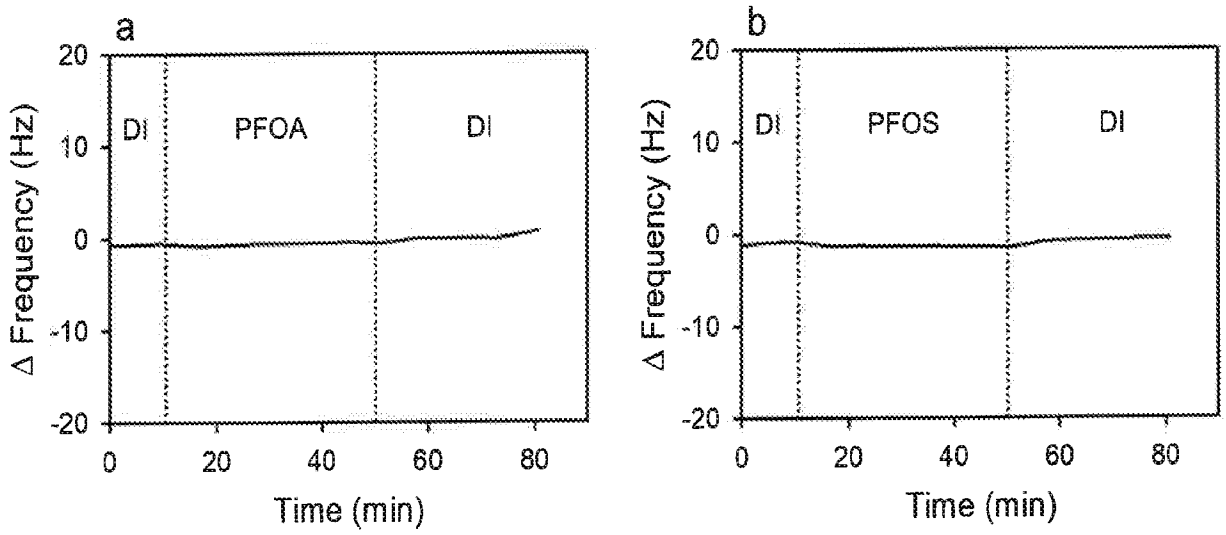
a
b
DI
PFOA
PFOS
Δ Frequency (Hz)
Time (min)

Fig. 13

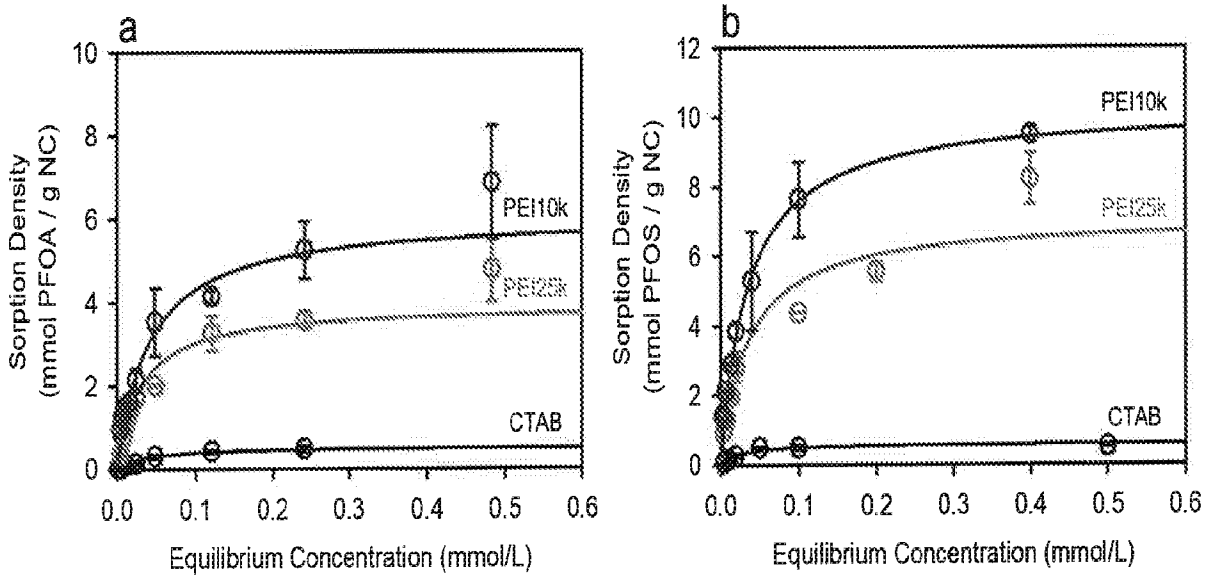
a
b
PEI10k
PEI25k
CTAB
Sorption Density (mmol PFOA / g NC)
Sorption Density (mmol PFOS / g NC)
Equilibrium Concentration (mmol/L)

Fig. 14

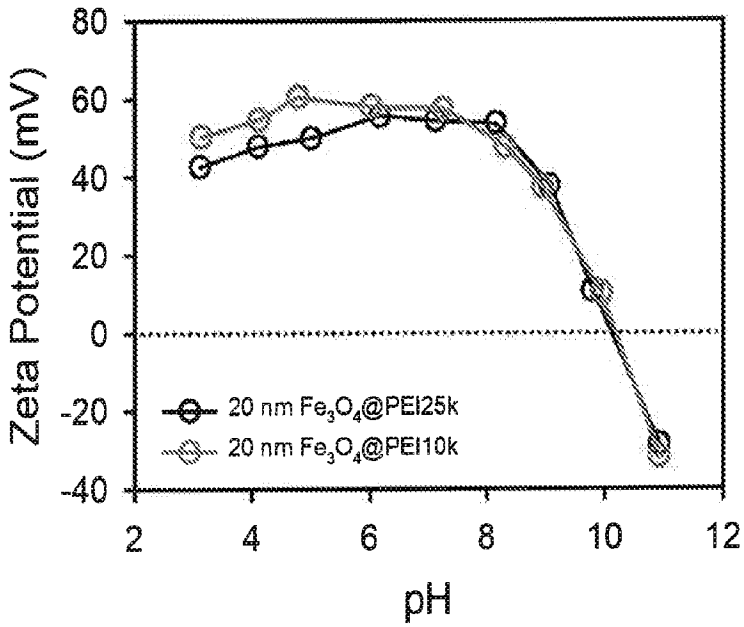
Zeta Potential (mV)
80
60
40
20
0
-20
-40
2
4
6
8
10
12
pH
20 nm Fe3O4@PEI25k
20 nm Fe3O4@PEI10k

Fig. 15

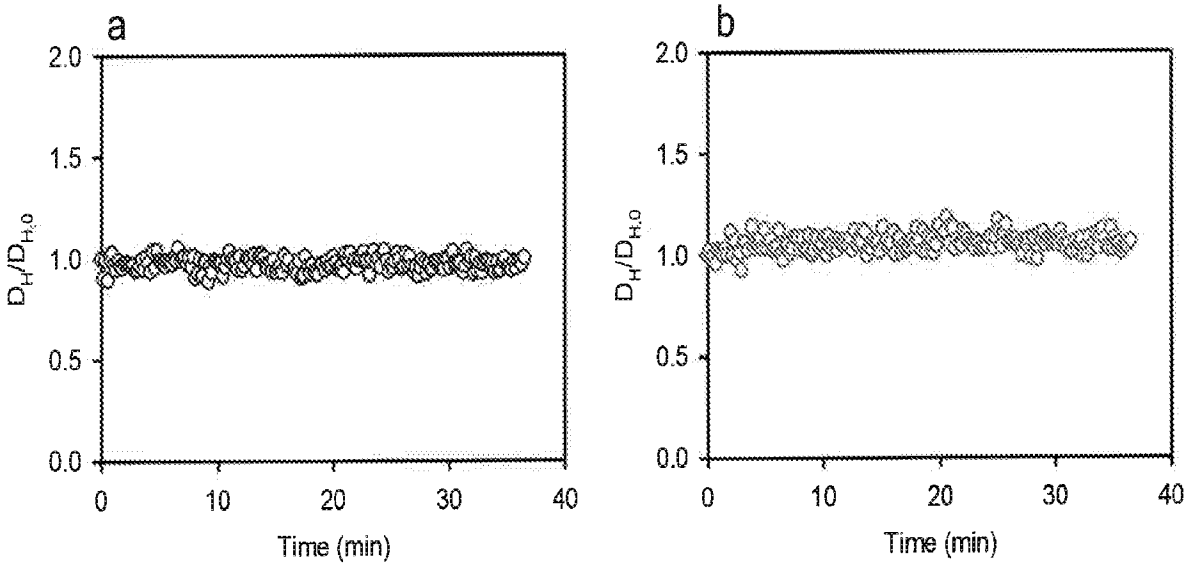
a
b
DH/DH,0
2.0
1.5
1.0
0.5
0.0
0
10
20
30
40
Time (min)

Fig. 16

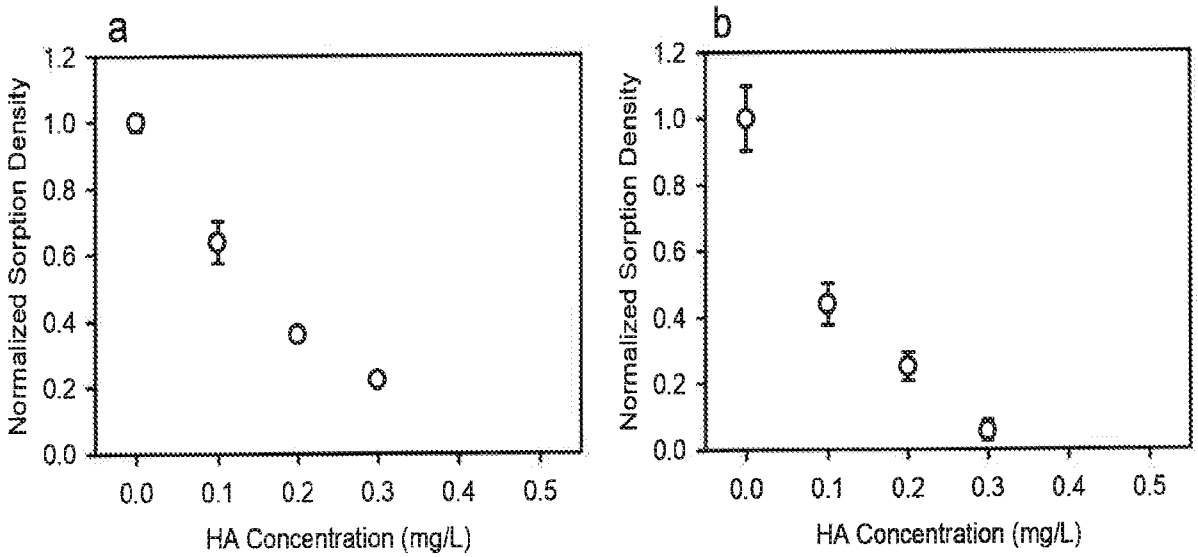
a
b
Normalized Sorption Density
HA Concentration (mg/L)
0.0
0.2
0.4
0.6
0.8
1.0
1.2
0.1
0.3
0.5

Fig. 17

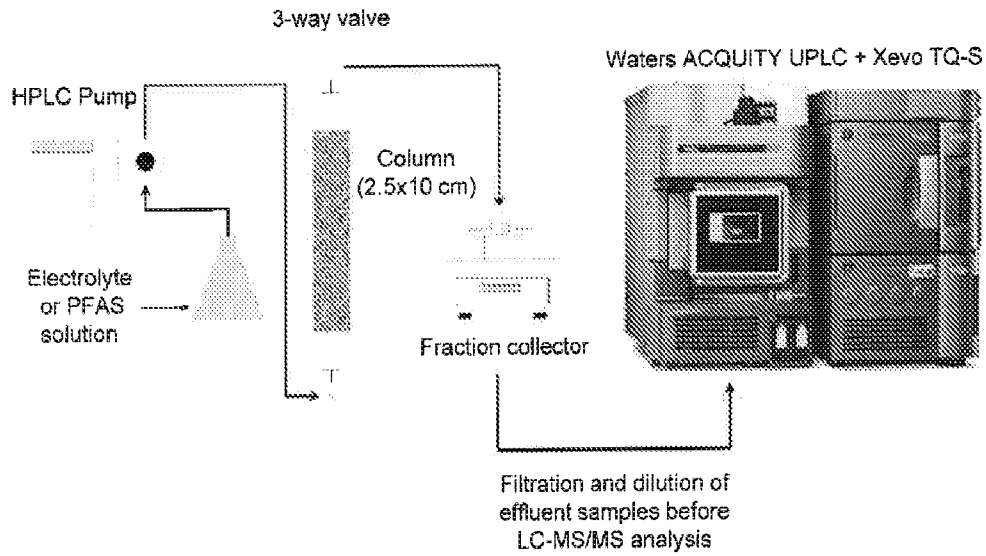
3-way valve
Waters ACQUITY UPLC + Xevo TQ-S
HPLC Pump
Column
(2.5x10 cm)
Electrolyte
or PFAS
solution
Fraction collector
Filtration and dilution of
effluent samples before
LC-MS/MS analysis

Fig. 18